

Urea Metal-organic Frameworks for Nitro-substituted compounds Sensing

*Alireza Azhdari Tehrani,^a Leili Esrafil, ^a Sedigheh Abedi,^a Ali Morsali,^{*a} Lucia Carlucci^b Davide M. Proserpio,^{b,c} Jun Wang,^d Peter C. Junk^d and Tianfu Liu^e*

^a*Department of Chemistry, Faculty of Sciences, Tarbiat Modares University, P.O. Box 14115-175, Tehran, Iran. E-mail: Morsali_a@modares.ac.ir;*

^b*Dipartimento di Chimica, Università degli Studi di Milano, Milano 20133, Italy*

^c*Samara Center for Theoretical Materials Science (SCTMS), Samara University, Samara 443086, Russia*

^d*College of Science & Engineering, James Cook University, Townsville Qld, 4811, Australia*

^e*Department of Chemistry, Northwestern University, 2145 Sheridan Road, Evanston, Illinois 60208-3113, USA*

Experimental Section.....	page 2
Synthesis of ligands, TMU-31 and TMU-32.....	page 3
ORTEP diagrams.....	page 6
Thermogravimetric analysis.....	page 7
FT-IR spectra.....	page 8
PXRD.....	page 9
N₂ adsorption-desorption.....	page 10
Solid state UV-vis.....	page 11
Fluorescence measurements.....	page 12
SEM images.....	page 30
Extraction.....	page 32
Theoretical calculations.....	page 36

Experimental Section

Materials and Physical Techniques

All starting materials, including Zinc(II) nitrate hexahydrate, 1,1'-Carbonyldiimidazole, 4,4'-oxybis(benzoic acid) (H₂OBA), 4-Aminobenzoic acid and 4-aminopyridine were purchased from Aldrich and Merck Company and used as received. Melting points were measured on an Electrothermal 9100 apparatus. IR spectra were recorded using Thermo Nicolet IR 100 FT-IR. The thermal behavior was measured with a PL-STA 1500 apparatus with the rate of 10°C.min⁻¹ in a static atmosphere of argon. X-ray powder diffraction (XRD) measurements were performed using a Philips X'pert diffractometer with mono chromated Cu-K α radiation. The ¹H-NMR spectrum was recorded on a Bruker AC-250 MHz spectrometer at ambient temperature in d₆-DMSO and D₂SO₄. The samples were also characterized by field emission scanning electron microscope (FE-SEM) SIGMA ZEISS and TESCAN MIRA with gold coating.

Single-Crystal Diffraction.

Single crystal of **TMU-31** was selected and mounted on a loop in inert oil and transferred to the cold gas stream of a Bruker APEX-II CCD diffractometer. The data was corrected for absorption and beam corrections based on the multi-scan technique as implemented in *SADABS*. The structures were solved by conventional methods and refined by full-matrix least-squares on all F^2 data using SHELX97 or SHELX2014 in conjunction with the X-Seed or Olex2 graphical user interface. Anisotropic thermal parameters were refined for non-hydrogen atoms and hydrogen atoms were calculated and refined with a riding model.

X-ray crystal structure determination for **TMU-32**: Crystals in viscous paraffin oil were mounted on cryoloops and intensity data were collected on the Australian Synchrotron MX1 beamline at 100 K with wavelength ($\lambda = 0.71073 \text{ \AA}$). The data were collected using the BlueIce^[1] GUI and processed with the XDS^[2] software package. The structures were solved by conventional methods and refined by full-matrix least-squares on all F^2 data using SHELX97^[3] or SHELX2014 in conjunction with the X-Seed^[4] or Olex2^[5] graphical user interface. Anisotropic thermal parameters were refined for non-hydrogen atoms and hydrogen atoms were calculated and refined with a riding model.

Crystallographic data: TMU-31: $C_{29}H_{27}N_7O_7Zn$, $M= 650.97 \text{ g mol}^{-1}$, Monoclinic, $P2_1/c$, $a= 11.6025(15) \text{ \AA}$, $b= 16.398(2) \text{ \AA}$, $c= 16.796(2) \text{ \AA}$, $\beta= 109.300(5)$, $V= 3016.0(7) \text{ \AA}^3$, $Z=4$, $\rho_{\text{calc}}= 1.434 \text{ g cm}^{-3}$, $\lambda= 1.54184$, $T=248 \text{ K}$, $R_1= 0.0494$, $wR_2= 0.1389$, $S=1.043$, $\text{ccdc}= 1493985$

PROBLEM: ALERT: The value of $\text{sine}(\text{theta_max})/\text{wavelength}$ is less than 0.550

RESPONSE: The crystals were small and diffracted weakly. Thus, data was truncated to include only the portion in which reflections were observed.

Crystallographic data: TMU-32: $C_{31}H_{34}N_6O_9Zn$, $M= 535.80 \text{ g mol}^{-1}$, Triclinic, $P\bar{1}$, $a= 8.9960(18) \text{ \AA}$, $b= 17.441(4) \text{ \AA}$, $c= 22.012(4) \text{ \AA}$, $\alpha= 111.09(3)^\circ$, $\beta= 96.09(3)^\circ$, $\gamma= 93.14(3)^\circ$, $V= 3188.0(13) \text{ \AA}^3$, $Z=4$, $\rho_{\text{calc}}= 1.116 \text{ g cm}^{-3}$, $\lambda= 0.71073$, $T=100 \text{ K}$, $R_1= 0.0992$, $wR_2= 0.2703$, $S= 1.088$, $\text{ccdc}= 1500658$

PROBLEM: ALERT: The ratio of given/expected molecular weight as calculated from the _atom_site* data lies outside the range $0.90 <> 1.10$

RESPONSE: The residual electron density in the lattice voids cannot be modelled as solvents thus the electron density in voids was accounted for using PLATON/S Each unit cell contains 8 DMF and 4 water molecules.

Synthesis

The synthesis of 4,4'-(carbonylbis(azanediyl))dibenzoic acid (L1) and 1,3-di(pyridin-4-yl)urea (L2) ligands was straightforward and was achieved in a few steps, starting from 4-aminobenzoic acid and 4-aminopyridine, respectively.

Synthesis of ligand L1

4-aminobenzoic acid (1.37 g, 10 mmol) was dissolved in a minimum amount of absolute ethanol (15 mL). As 1 mL of concentrated sulfuric acid was added, a white suspension formed which was vigorously stirred and refluxed for 3 h to give a clear solution. The reaction mixture was cooled to 40°C and poured into a saturated solution of sodium bicarbonate in water (100 mL). Vigorous effervescence was observed with the precipitation of a white solid. The precipitate was filtered and dried in air at room temperature (**1**). Ethyl 4-aminobenzoate (1.65 g, 10 mmol) was dissolved in 25 mL of dry THF with stirring. To this solution, 1,1'-Carbonyldiimidazole (0.97 g 6 mmol) was added. The mixture was refluxed under argon atmosphere overnight. The mixture was cooled to room temperature and the solvent was removed in vacuo. The resulting residue

was taken up in ethyl acetate, washed with 1M HCl and brine (3 times), dried over MgSO_4 and concentrated to afford 1.33 g (75%) of **2** as a white powder. To a 100 mL round-bottom flask was added **2** (3.56 g, 10 mmol) and potassium hydroxide (4.0 g, 0.072 mol) in methanol (30 mL). The mixture was stirred vigorously and refluxed. A white precipitate appeared after about an hour, and this mixture was refluxed for an additional 5 h. The precipitate was filtered and washed several times with distilled water and dried in vacuo to give **3** (2.4 g, 82% yield).

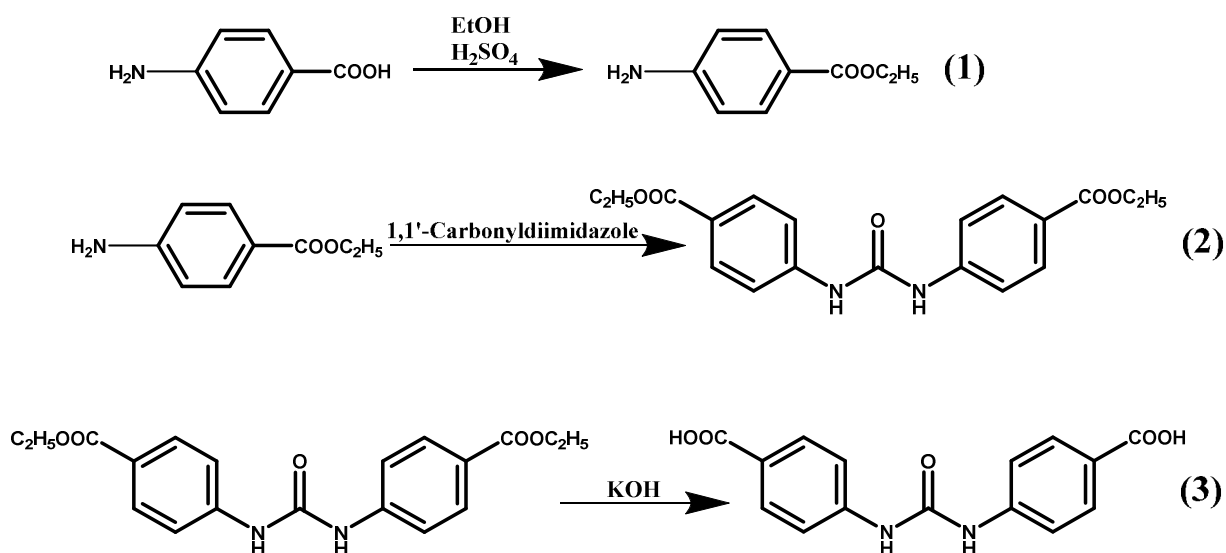


Figure S1. Synthesis of L1

Spectroscopic data:

(1): (M.p. 88-90°C), FT-IR (KBr pellet, cm^{-1}): 3421, 3342, 3223, 2978, 1685, 1597, 1512, 1280, 1169, 1119, 1023, 847, 772, 698. Anal. calcd for $\text{C}_9\text{H}_{11}\text{NO}_2$: C, 65.44; H, 6.71; N, 8.48, Found: C, 65.36; H, 6.59, N: 8.14. MS (m/z): 165.1 (M^+ , base peak), 137.1.

(2): FT-IR (KBr pellet, cm^{-1}): 3322 (s), 2979 (w), 1711 (vs), 1652 (s), 1600 (s), 1553 (s), 1405 (w), 1280 (s), 1170 (m), 1021(m), 767 (m), 637 (m). Anal. calcd for $\text{C}_{19}\text{H}_{20}\text{N}_2\text{O}_5$: C, 64.04; H, 5.66; N: 7.86, Found: C, 63.94; H, 5.52, N: 7.80. MS (m/z): 356.5 (M^+ , base peak), 311.4, 191.3.

(3): FT-IR (KBr pellet, cm^{-1}): 3318 (s), 2845 (w), 2667 (w), 2554 (w), 1668 (vs), 1593 (m), 1537 (vs), 1419 (m), 1303 (s), 1224 (s), 1177 (m), 935 (w), 862(w), 762 (w), 547 (w). Anal. calcd for $\text{C}_{15}\text{H}_{12}\text{N}_2\text{O}_5$: C, 60.00; H, 4.03; N: 9.33, Found: C, 59.56; H, 3.92, N: 9.12. MS (m/z):

300.1 (M⁺, base peak), 256.2, 212.2. ¹H-NMR (d₆-DMSO) 12.61 (2H, d), 9.19 (2H, s), 7.88-7.92 (4H, d), 7.58-7.61 (4H, d).

Synthesis of ligand L2

4-aminopyridine (0.941 g, 10 mmol) was dissolved in 25 mL of dry THF. To this solution, 1,1'-Carbonyldiimidazole (0.97 g 6 mmol) was added. The mixture was refluxed under argon atmosphere overnight. The mixture was cooled to room temperature and the solvent was removed in vacuo. The resulting residue was taken up in brine and washed several times with distilled water and dried in vacuo to give white precipitate.

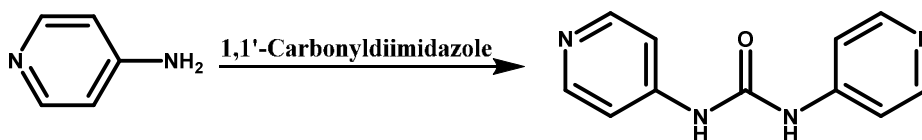


Figure S2. Synthesis of L2

Spectroscopic data:

FT-IR (KBr pellet, cm⁻¹): 3394-2938 (vs), 2490 (m), 2283 (w), 2221 (m), 1734 (s), 1591 (vs), 1505 (vs), 1420 (m), 1331 (m), 1283 (s), 1188 (vs), 1000 (m), 826(s), 732 (w), 524 (w). Anal. calcd for C₁₁H₁₀N₄O: C, 61.67; H, 4.71; N, 26.15, Found: C, 60.58; H, 4.64, N: 26.28. MS (m/z): 214.10 (M⁺, base peak). ¹H-NMR (d₆-DMSO) 9.29 (2H, s), 8.37-8.38 (4H, d), 7.43-7.44 (4H, d).

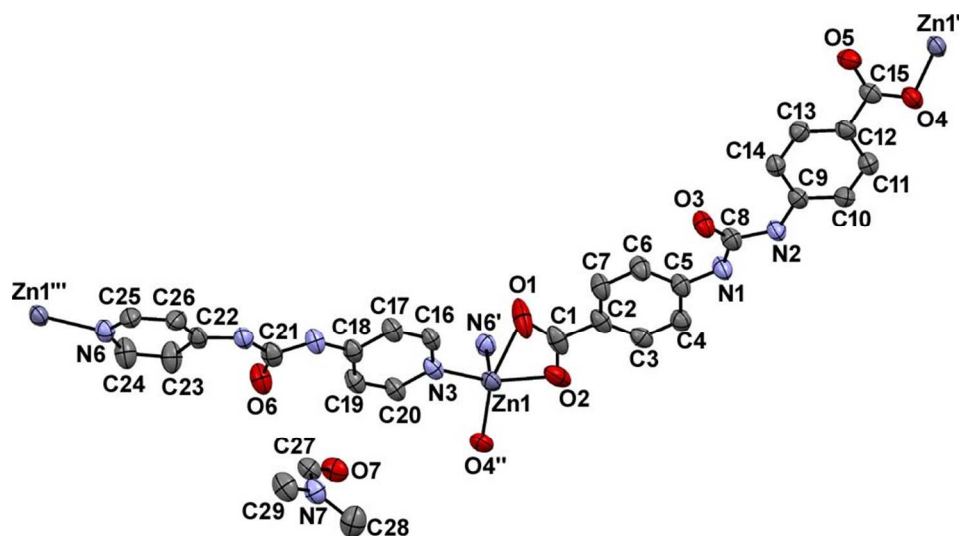


Figure S3: Ortep view of the asymmetric unit of **TMU-31** showing coordination environment about Zn1. Thermal ellipsoids are drawn at 50% of probability, hydrogen atoms are omitted for clarity. Symmetry codes: (') $1+x, 1.5-y, 1/2+z$; (") $-1+x, 1.5-y, 1/2+z$; (""') $-1+x, 1/2-y, -1/2+z$.

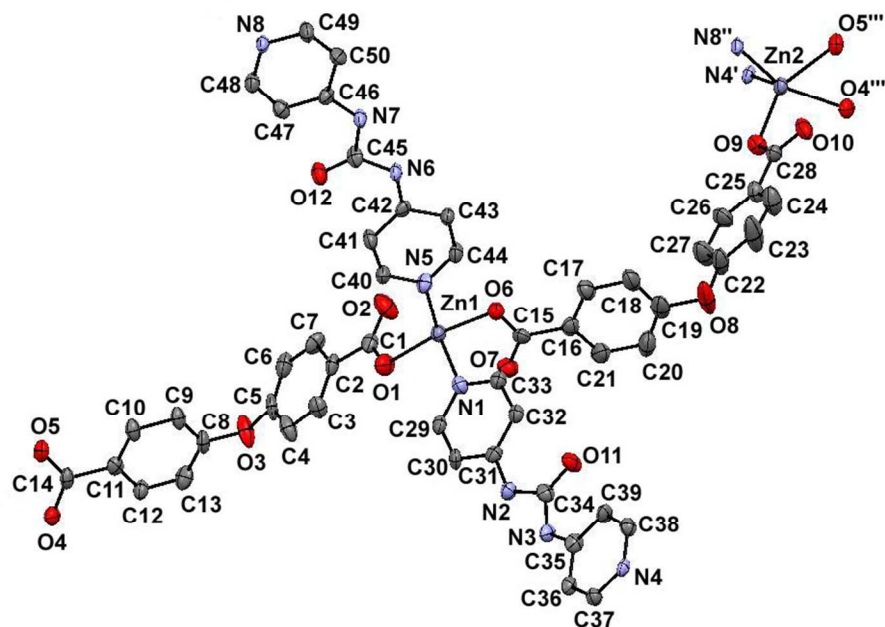


Figure S4; Ortep view of the asymmetric unit of **TMU-32** showing coordination environment about Zn1 and Zn2. Thermal ellipsoids are drawn at 50% of probability, hydrogen atoms are omitted for clarity. Symmetry codes: (') $x, y, -1+z$; (") $2-x, -y, 1-z$; (""') $-2+x, -1+y, -1+z$.

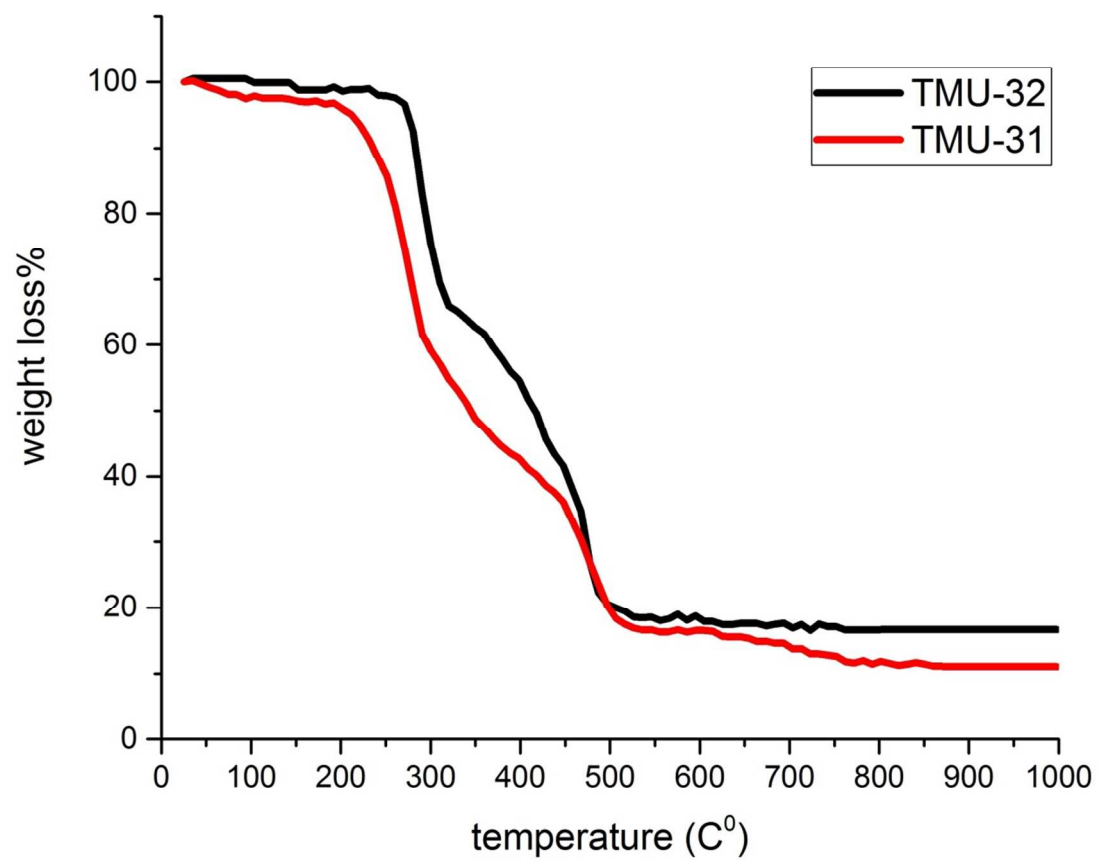


Figure S5. Thermogravimetric analysis of **TMU-31** and **TMU-32**

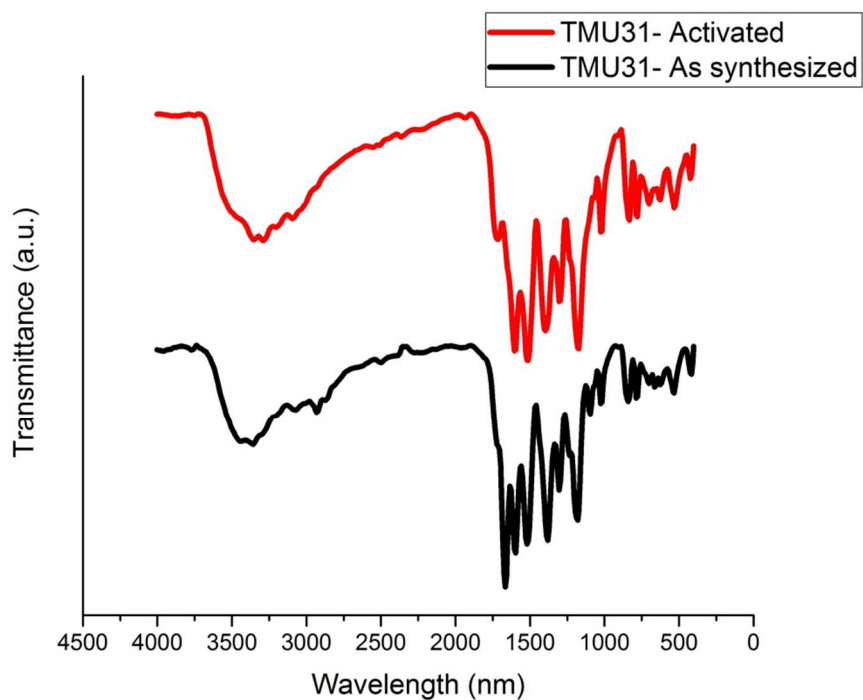


Figure S6. FT-IR spectra of **TMU-31**

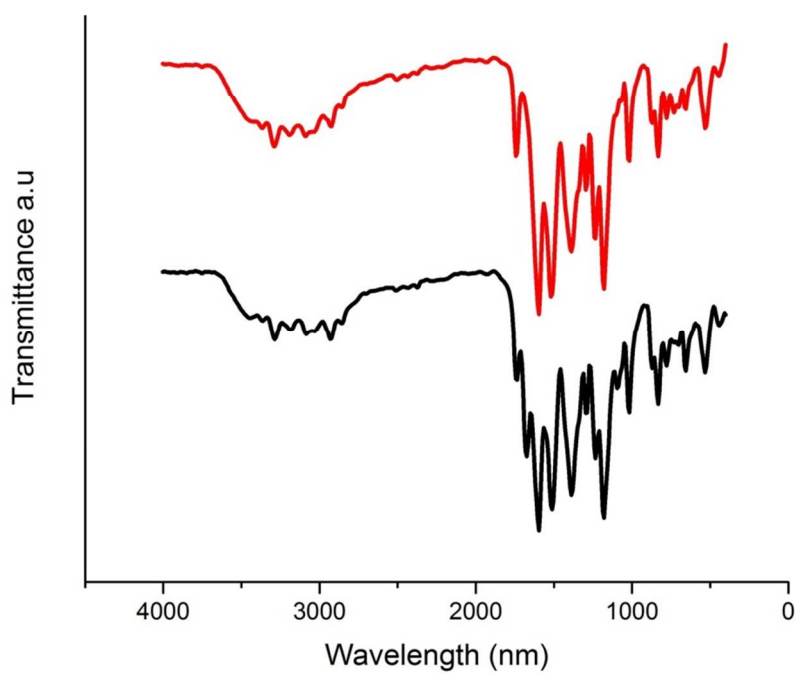


Figure S7. FT-IR spectra of as-synthesized (black) and activated (red) **TMU-32**

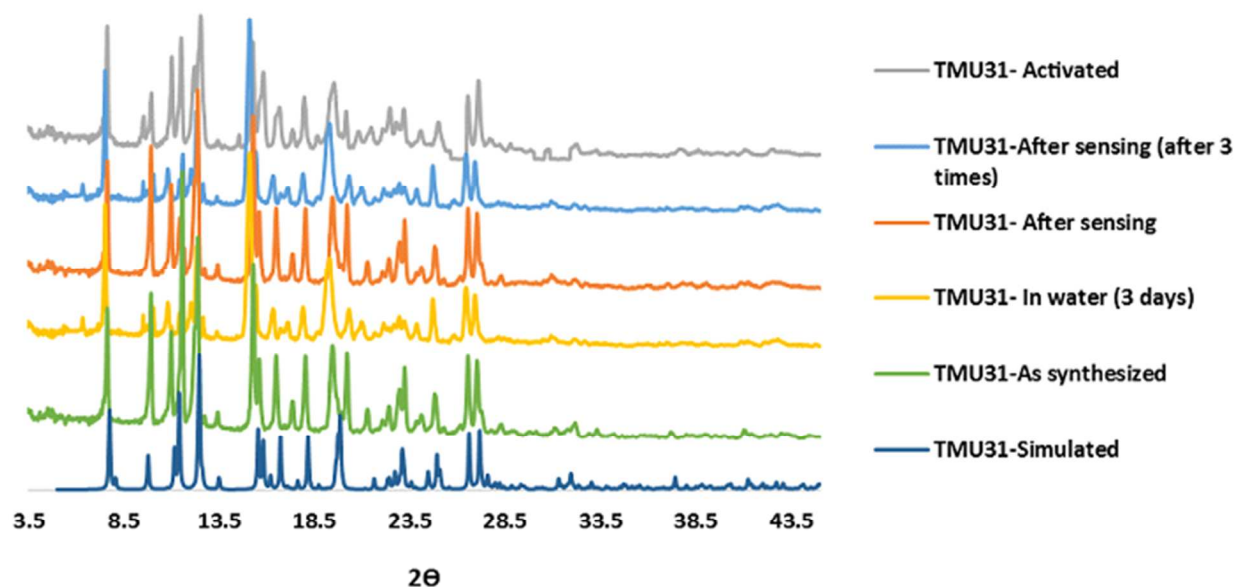


Figure S8. PXRD patterns of simulated, as-synthesized, stabilities in different solvents, after sensing and activated form of **TMU-31**

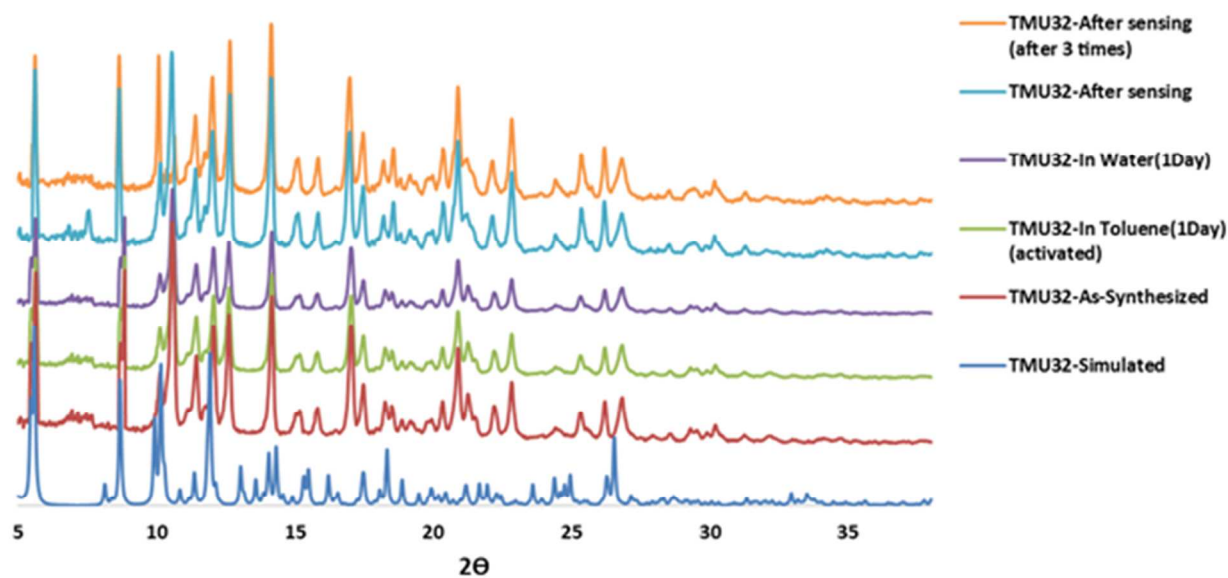


Figure S9. PXRD patterns of simulated, as-synthesized, stabilities in water and toluene (activated sample) and after sensing form of **TMU-32**

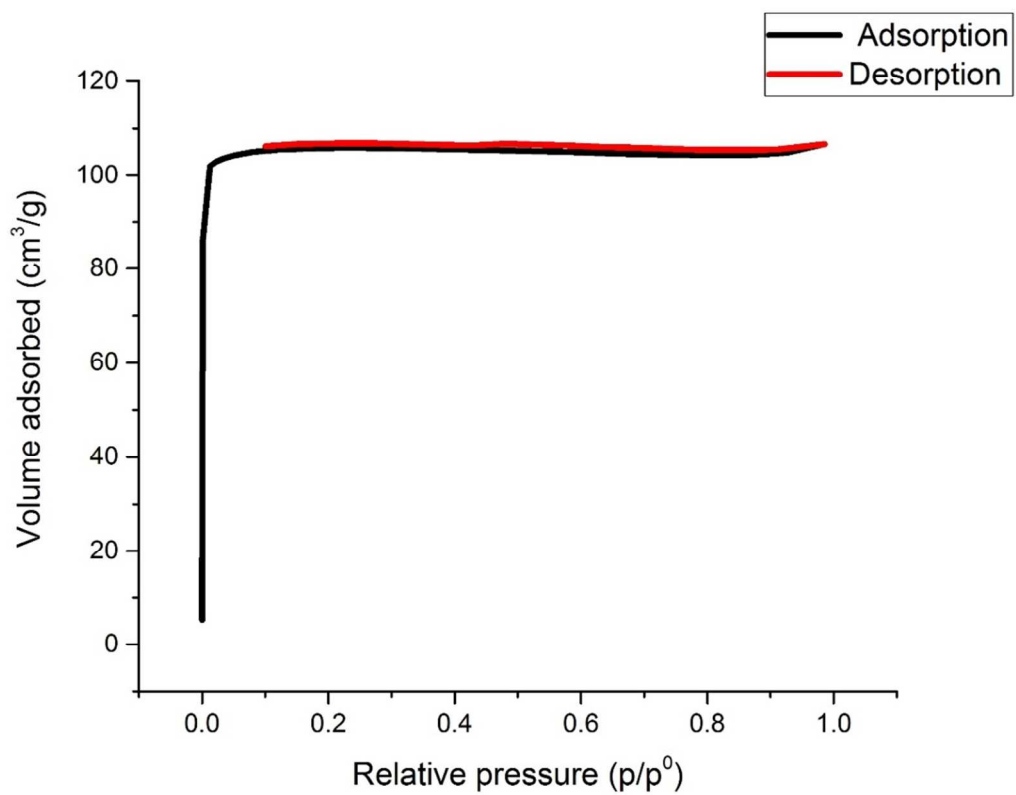


Figure S10. N₂ adsorption and desorption isotherms for TMU-32 at 77 K

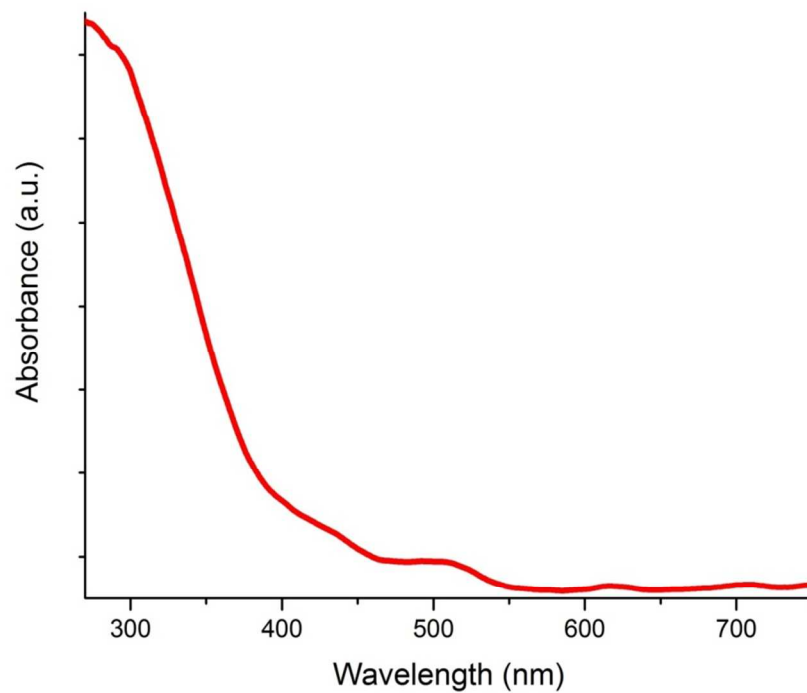


Figure **S11**. Solid state UV-vis spectroscopy of **TMU-31**.

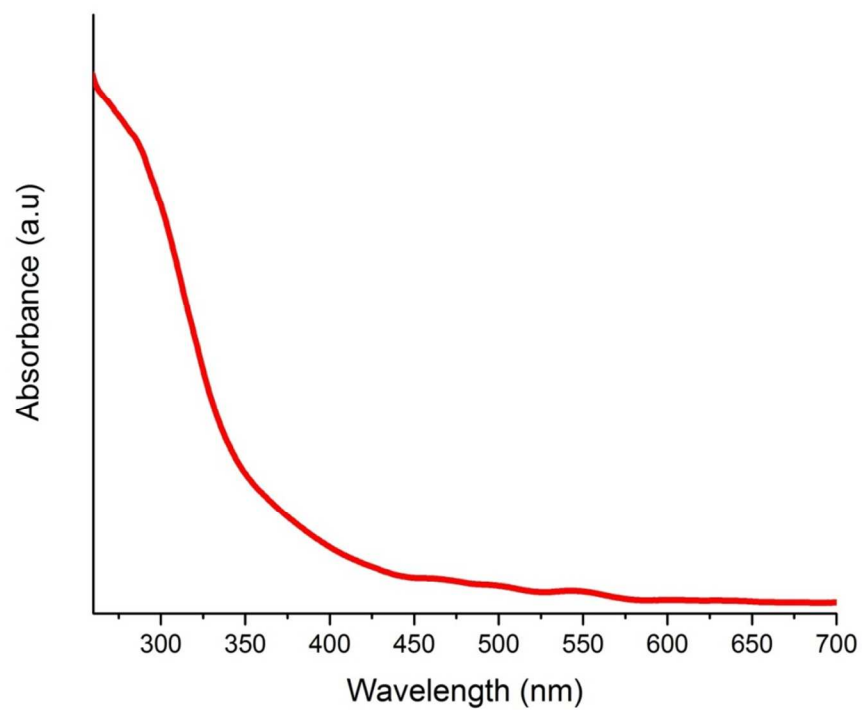


Figure **S12**. Solid state UV-vis spectroscopy of **TMU-32**

Fluorescence Measurements

The Fluorescence properties of TMU-31 and TMU-32 were measured in different solvent emulsions containing MOFs using a PerkinElmer-LS55 Fluorescence Spectrometer at room temperature. In a typical procedure, 1 mg of an activated MOF was grinded down, and then immersed in different analyte solutions (4 ml) and after 1 hours was tested in the emission mode. For fluorescence measurement in the presence of nitroaromatic compounds toluene was chosen as suitable solvent.

Stern-Volmer Plots

According to the Stern-Volmer equation, $(I_0/I) = K_{SV} [A] + 1$, Where here, I_0 is the initial fluorescence intensity of soaked MOF sample in toluene, I is the fluorescence intensity in the presence of analyte, $[A]$ is the molar concentration of analyte, and K_{SV} is the Stern-Volmer constant (M^{-1}). For the quenching constant extraction, emission intensity of MOFs was recorded by suspending them into different concentrations of analyte solutions in toluene, upon the same manner described in Fluorescence measurement section.

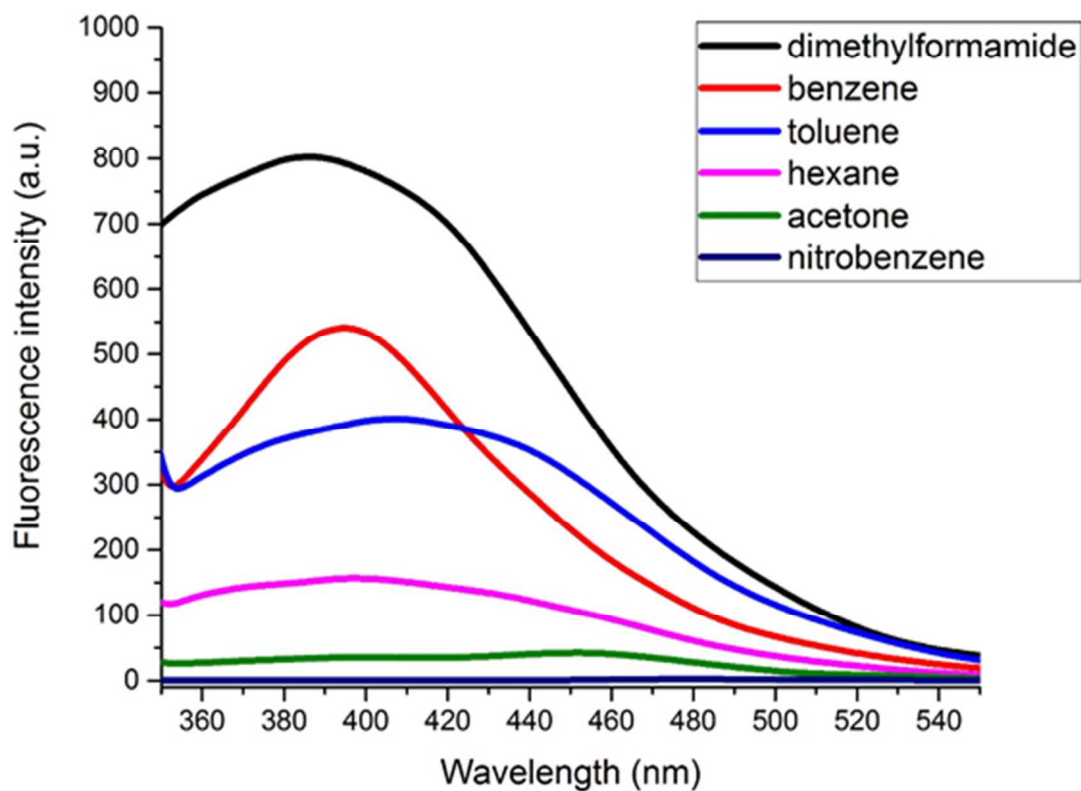


Figure S13. Fluorescence emission spectra of **TMU-31** dispersed in different solvents

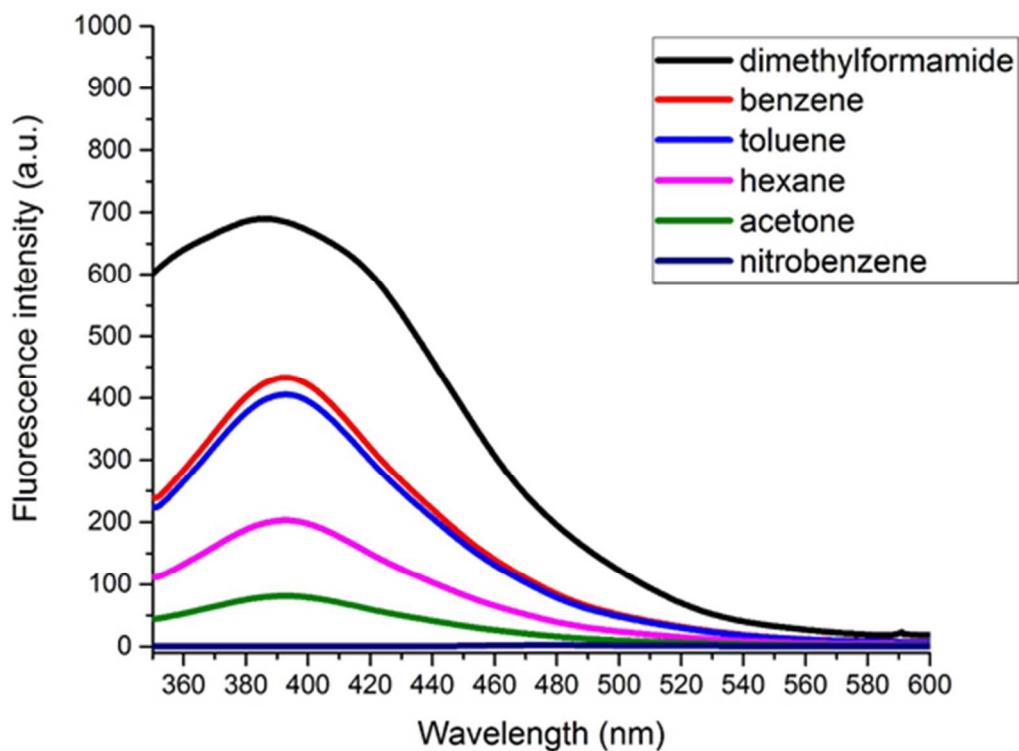


Figure S14. Fluorescence emission spectra of **TMU-32** dispersed in different solvents

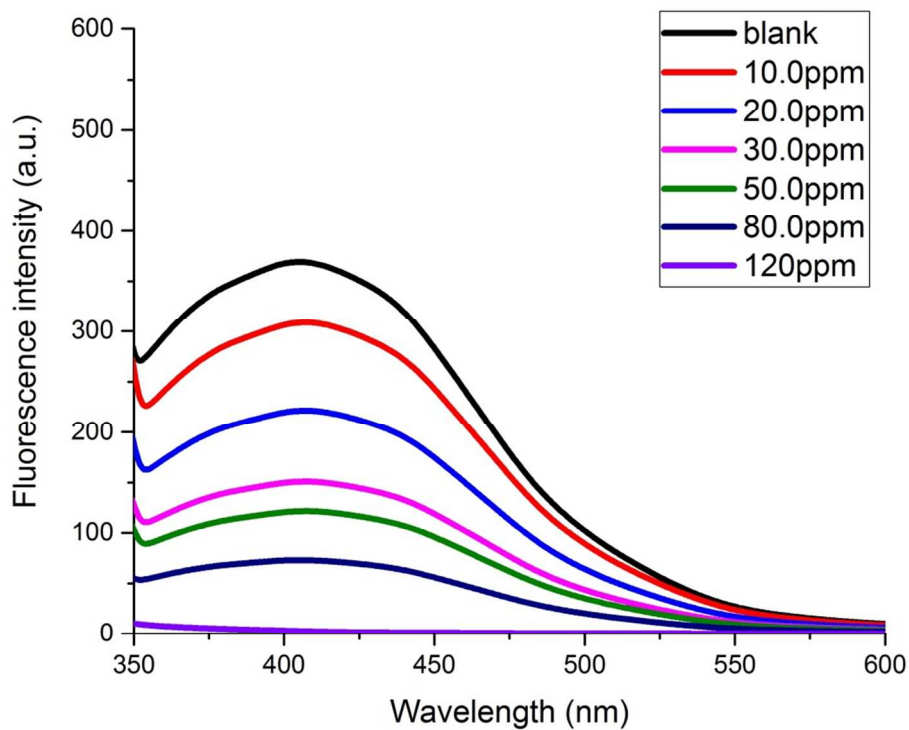


Figure S15. Fluorescence emission spectra of **TMU-31** dispersed in toluene solution at different concentrations of **NB**, excited at 320 nm.

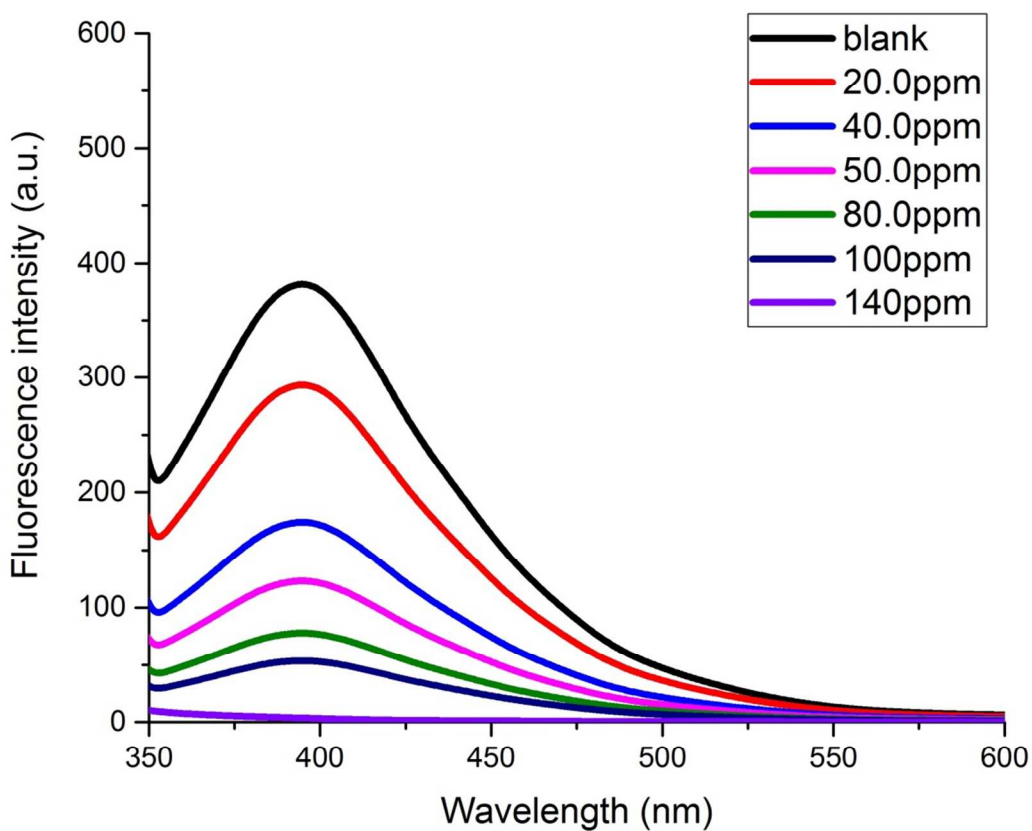


Figure S16. Fluorescence emission spectra of **TMU-32** dispersed in toluene solution at different concentrations of **NB**, excited at 320 nm.

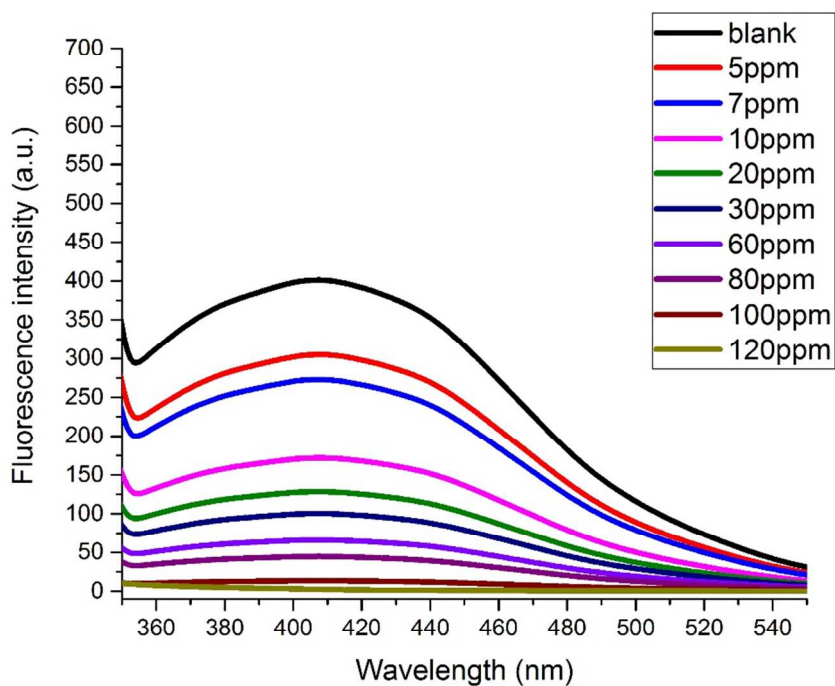


Figure S17. Fluorescence emission spectra of **TMU-31** dispersed in toluene solution at different concentrations of **1,3-DNB**, excited at 320 nm.

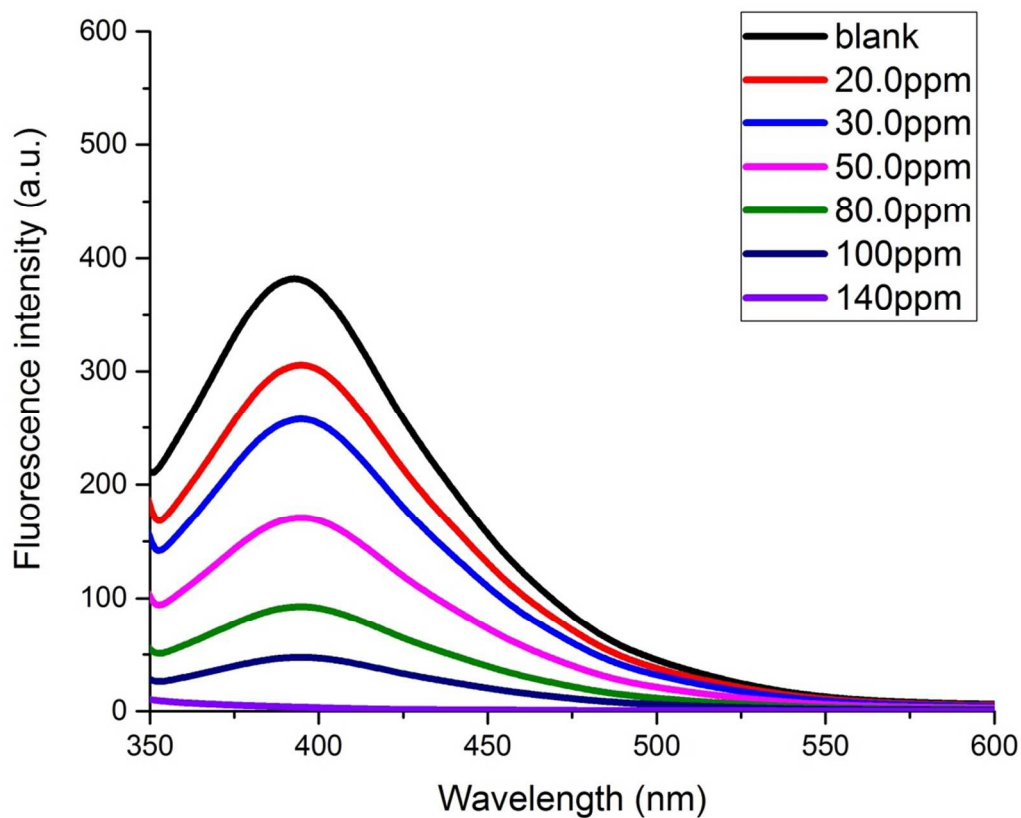


Figure S18. Fluorescence emission spectra of **TMU-32** dispersed in toluene solution at different concentrations of **1,3-DNB**, excited at 320 nm.

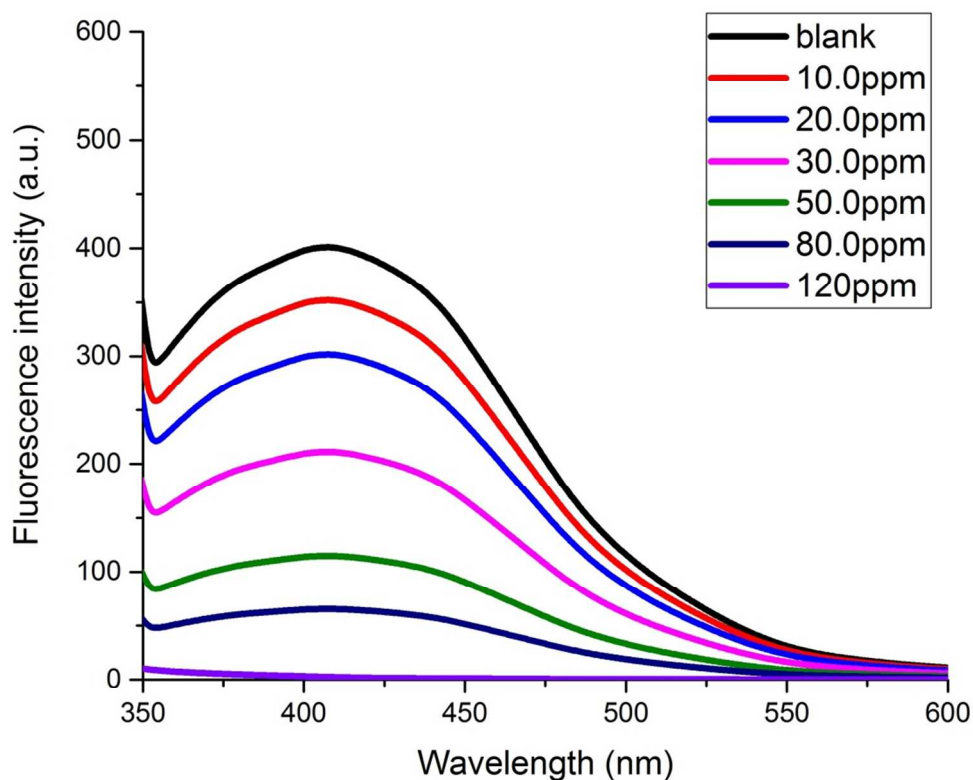


Figure S19. Fluorescence emission spectra of **TMU-31** dispersed in toluene solution at different concentrations of **2,4-DNT**, excited at 320 nm.

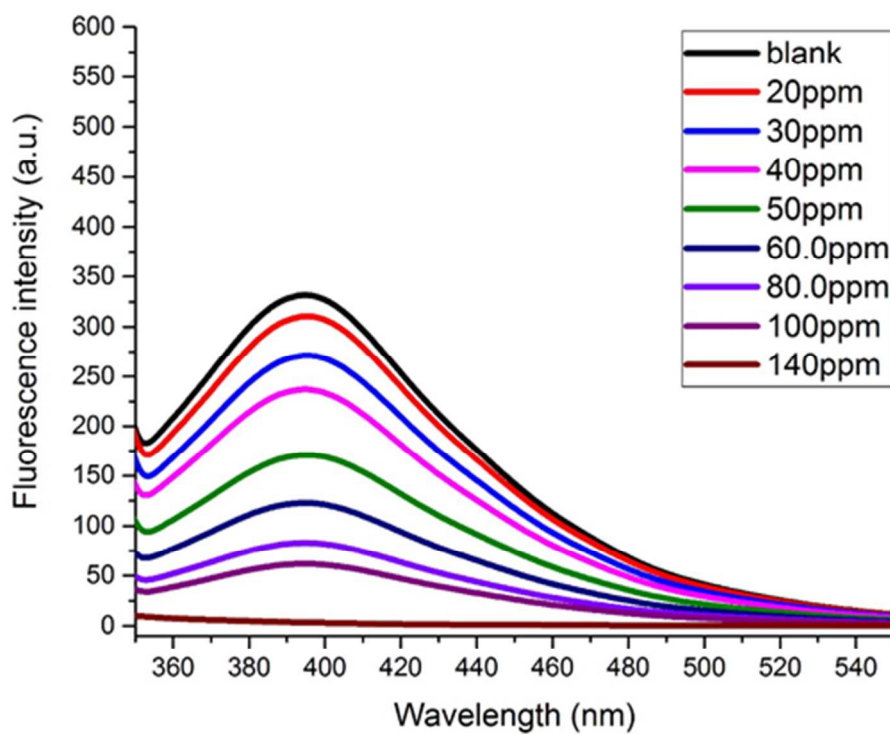


Figure S20. Fluorescence emission spectra of **TMU-32** dispersed in toluene solution at different concentrations of **2,4-DNT**, excited at 320 nm.

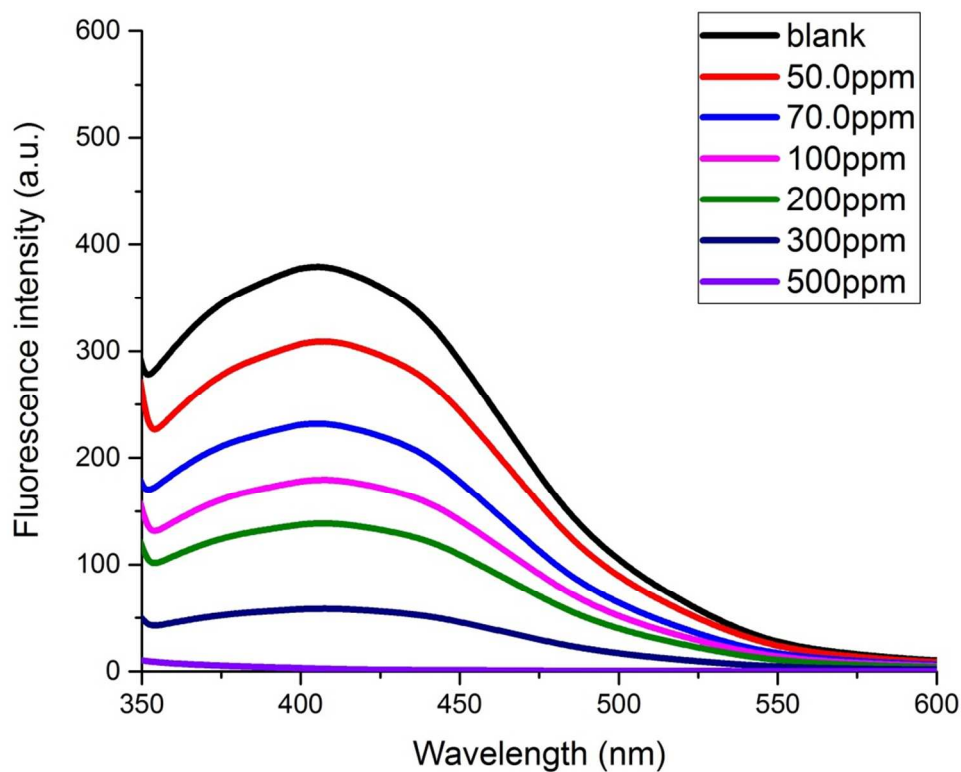


Figure S21. Fluorescence emission spectra of **TMU-31** dispersed in toluene solution at different concentrations of **TNT**, excited at 320 nm.

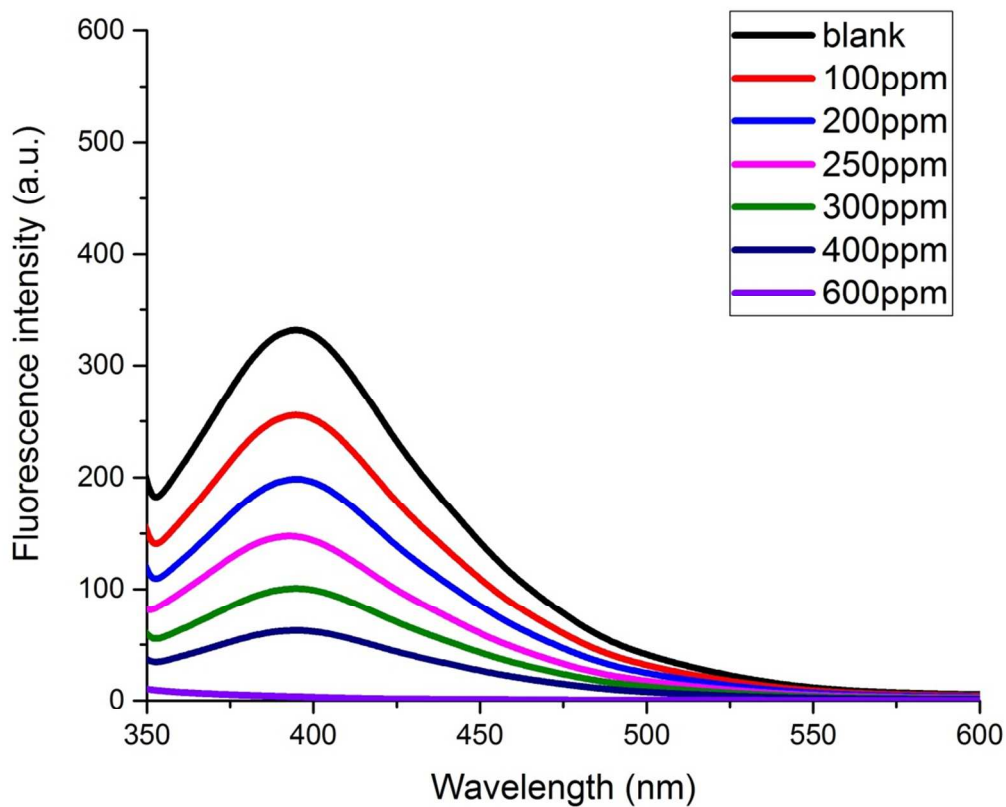


Figure S22. Fluorescence emission spectra of **TMU-32** dispersed in toluene solution at different concentrations of **TNT**, excited at 320 nm.

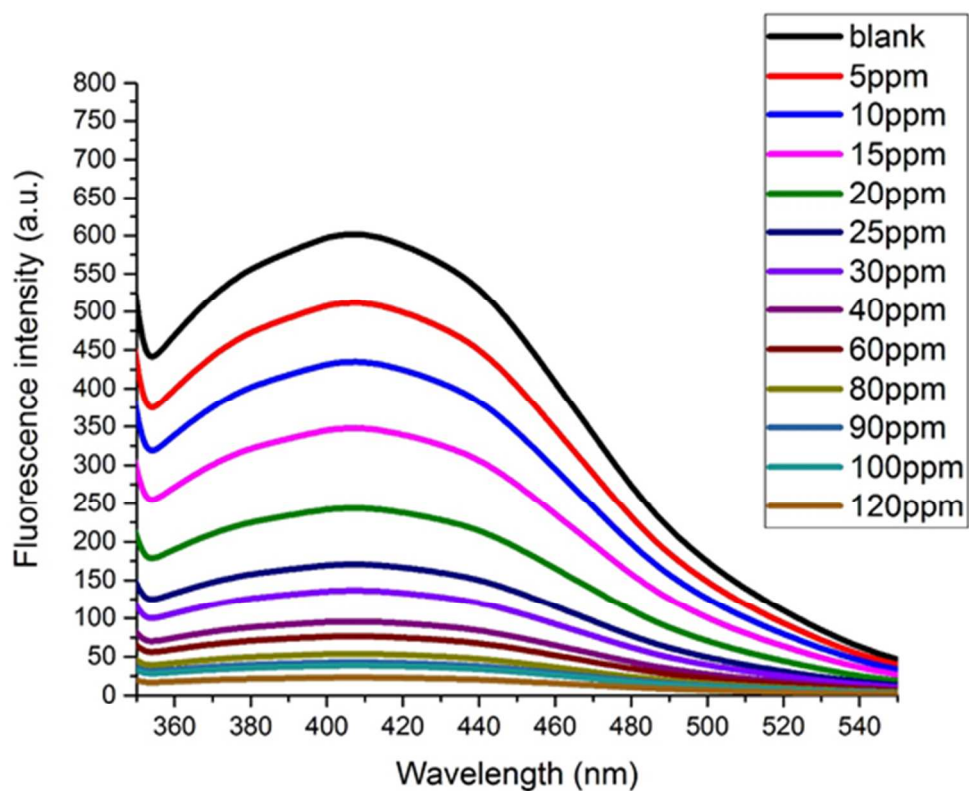


Figure S23. Fluorescence emission spectra of **TMU-31** dispersed in toluene solution at different concentrations of **NM**, excited at 320 nm.

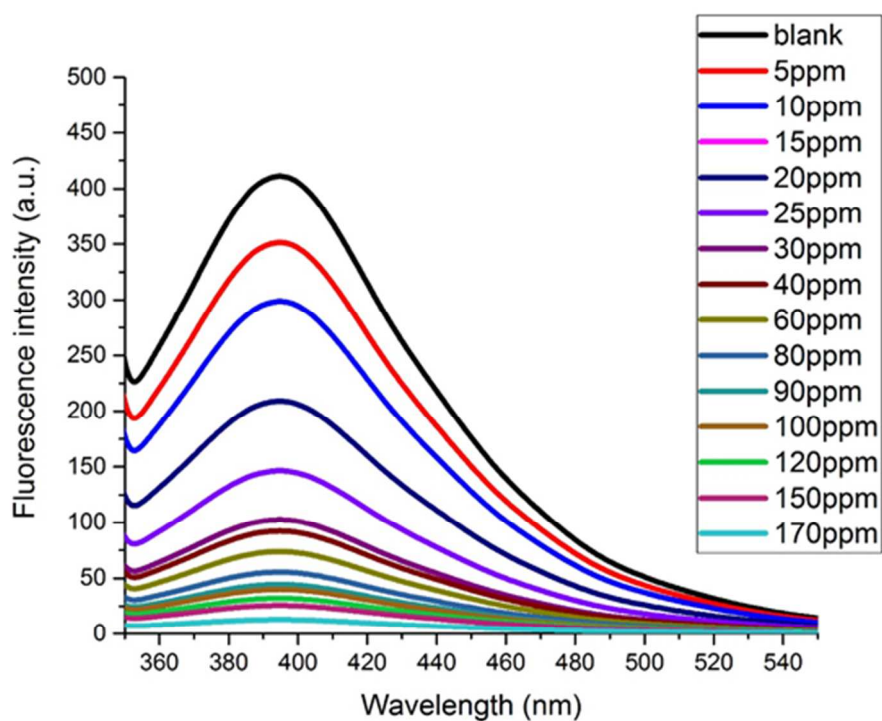
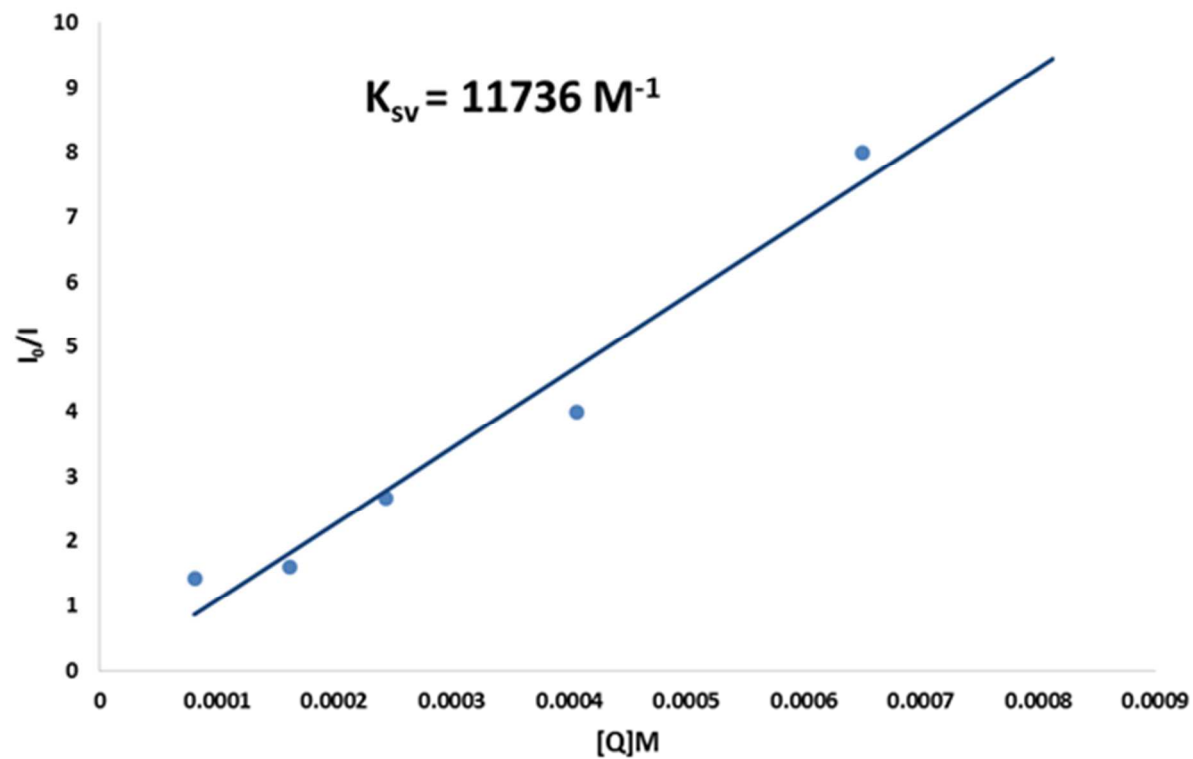
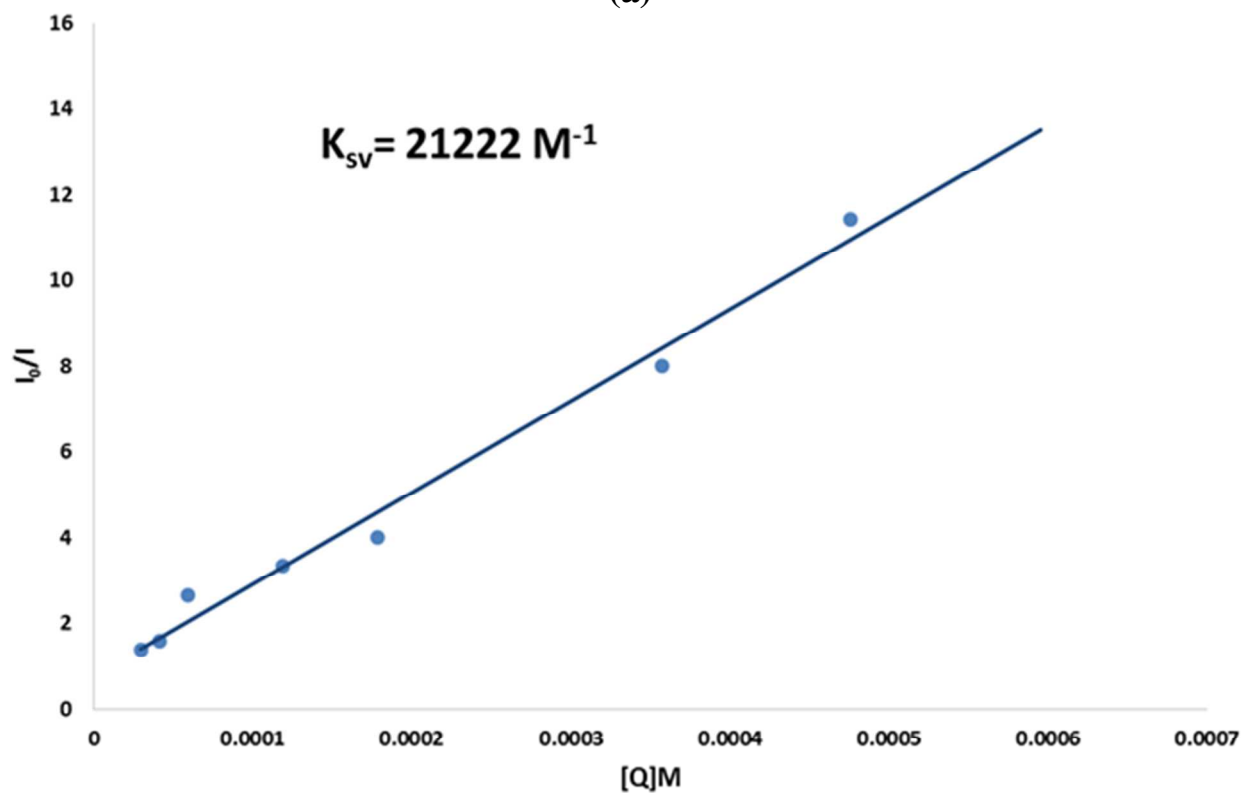


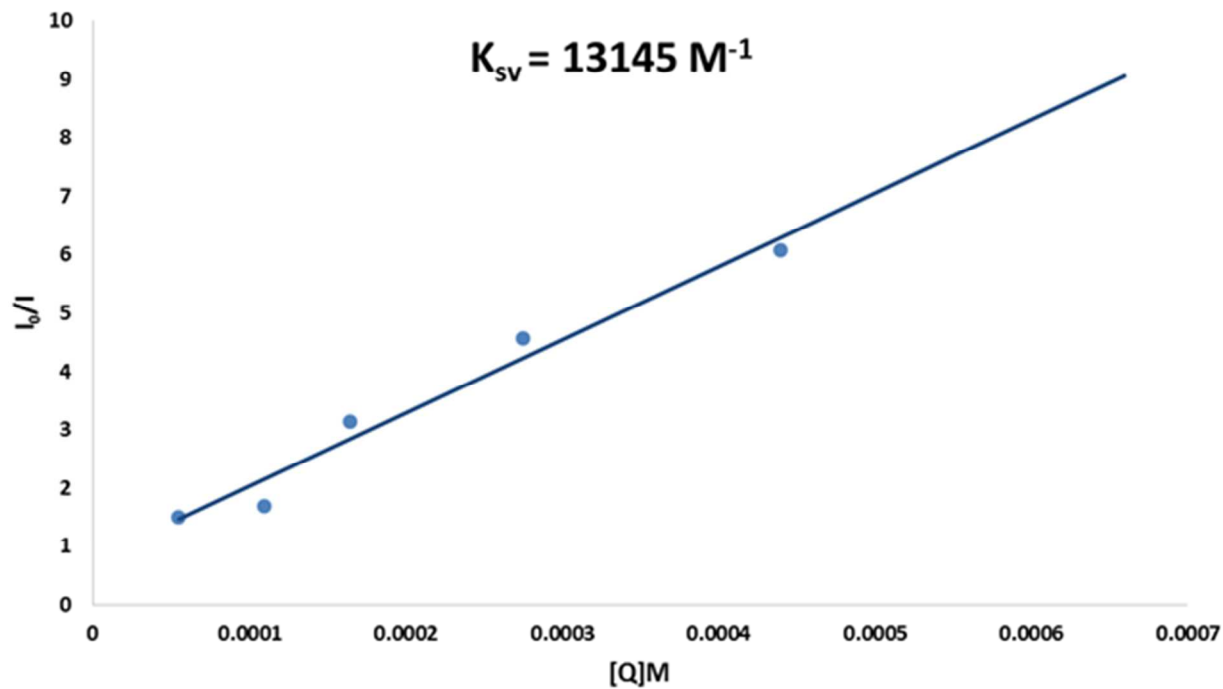
Figure S24. Fluorescence emission spectra of **TMU-32** dispersed in toluene solution at different concentrations of **NM**, excited at 320 nm.



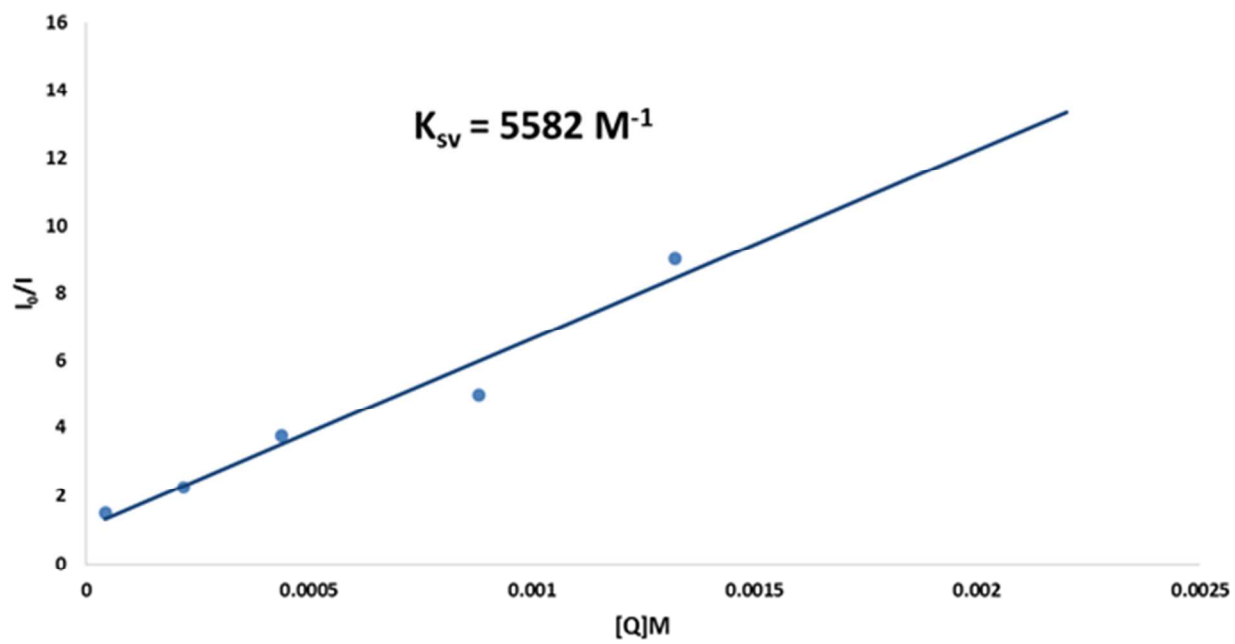
(a)



(b)



(c)



(d)

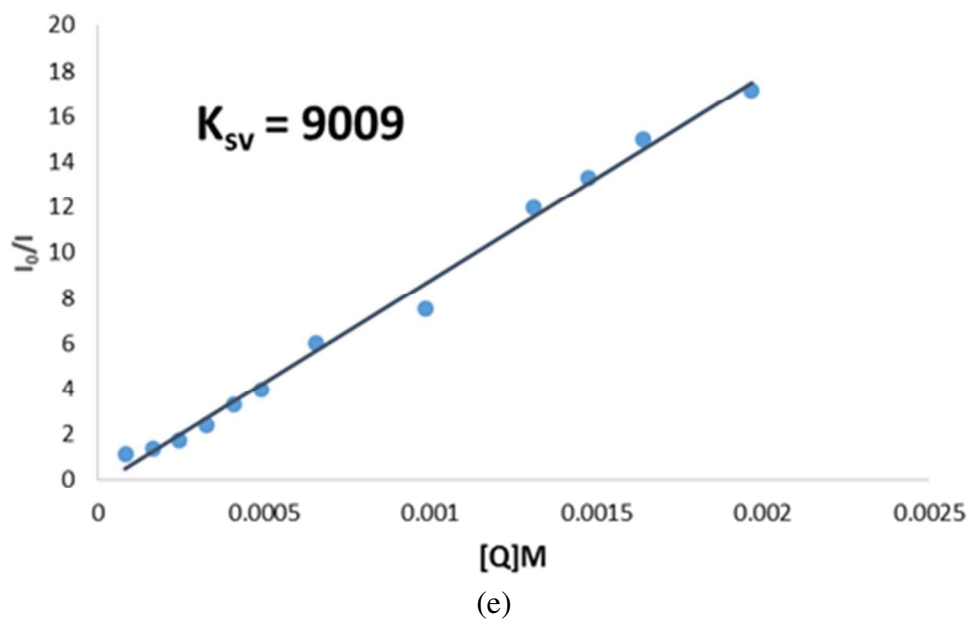
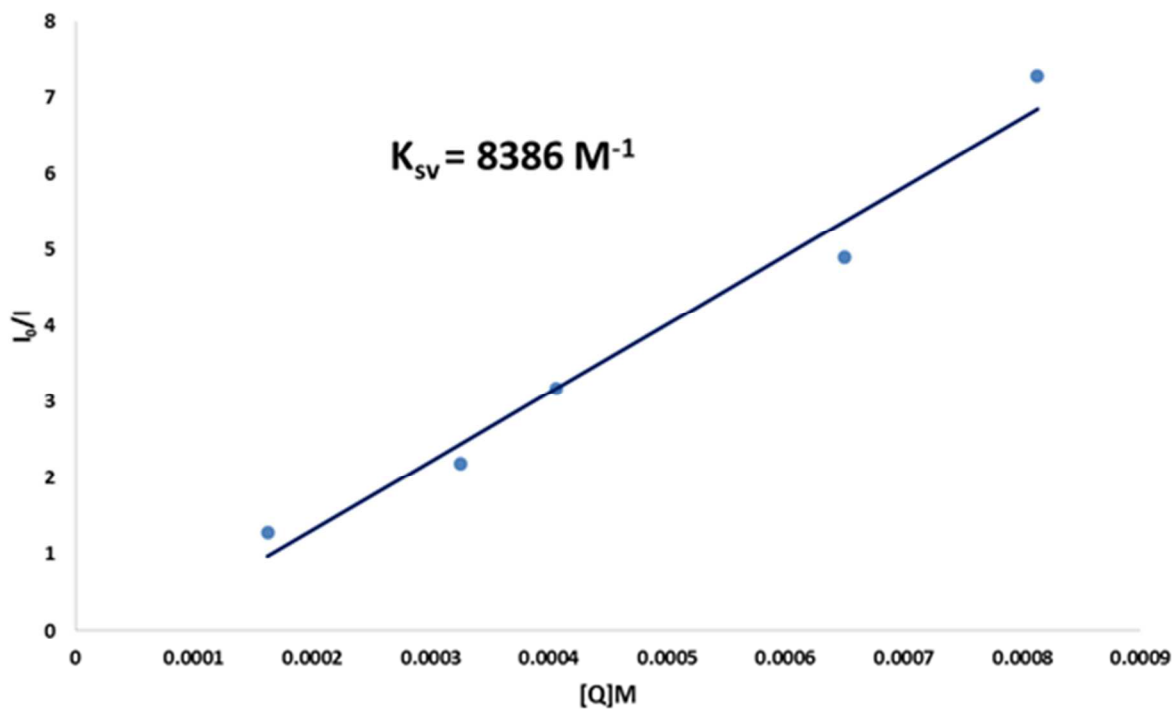
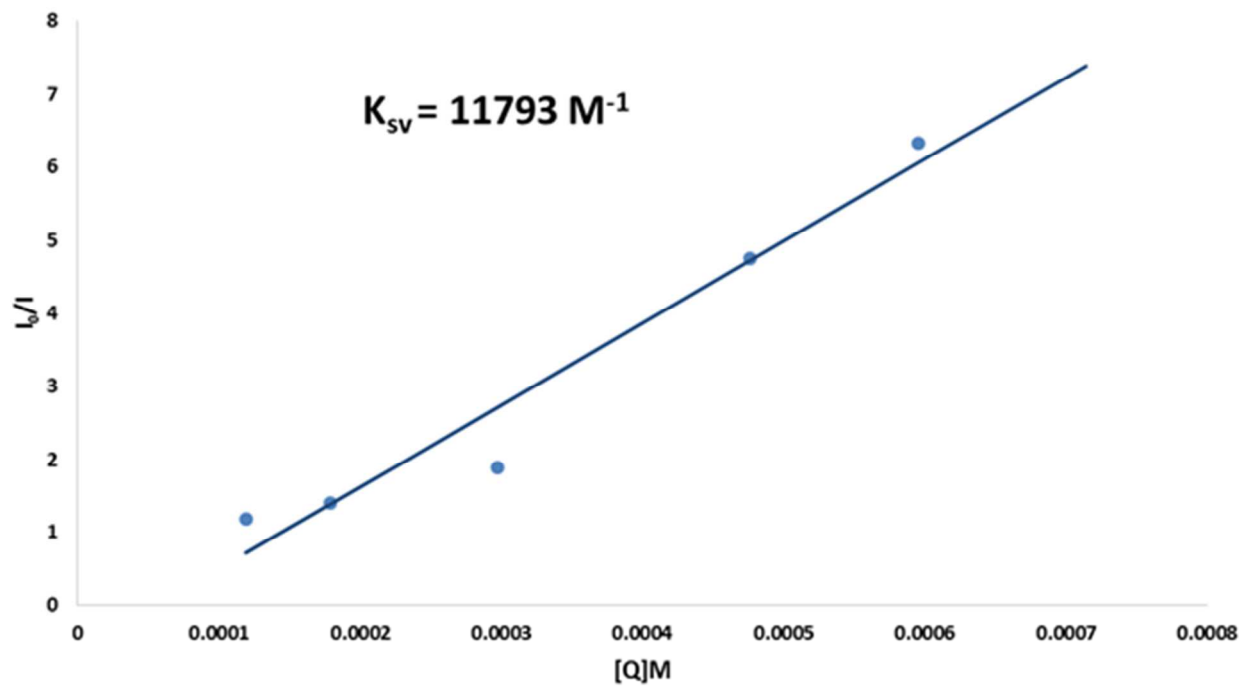


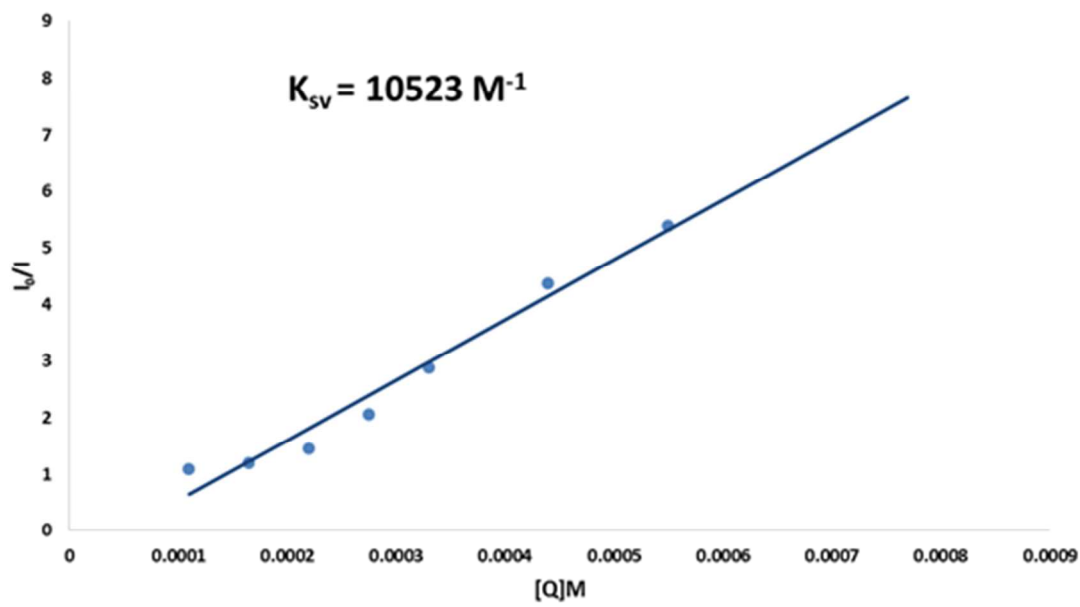
Figure S25. Stern–Volmer (SV) plots in the presence of 1 mg of **TMU-31** in different **NB** (a) **1,3-DNB** (b) **2,4-DNT** (c) **TNT** (d) **NM** (e) concentrations ($[Q]$) in toluene.



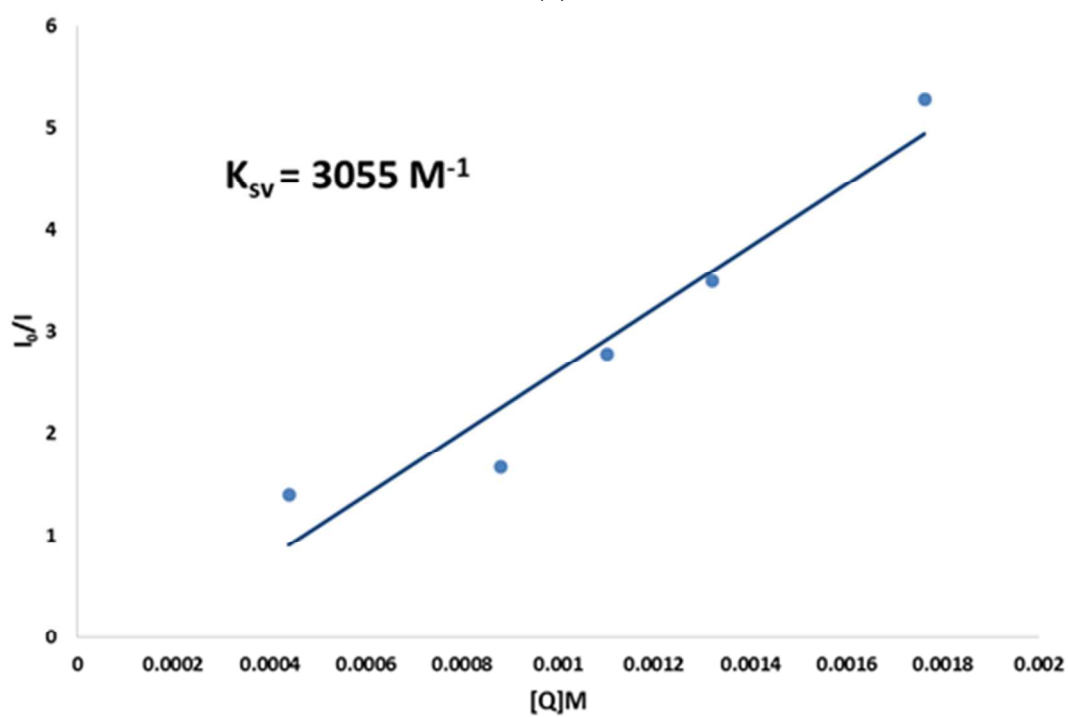
(a)



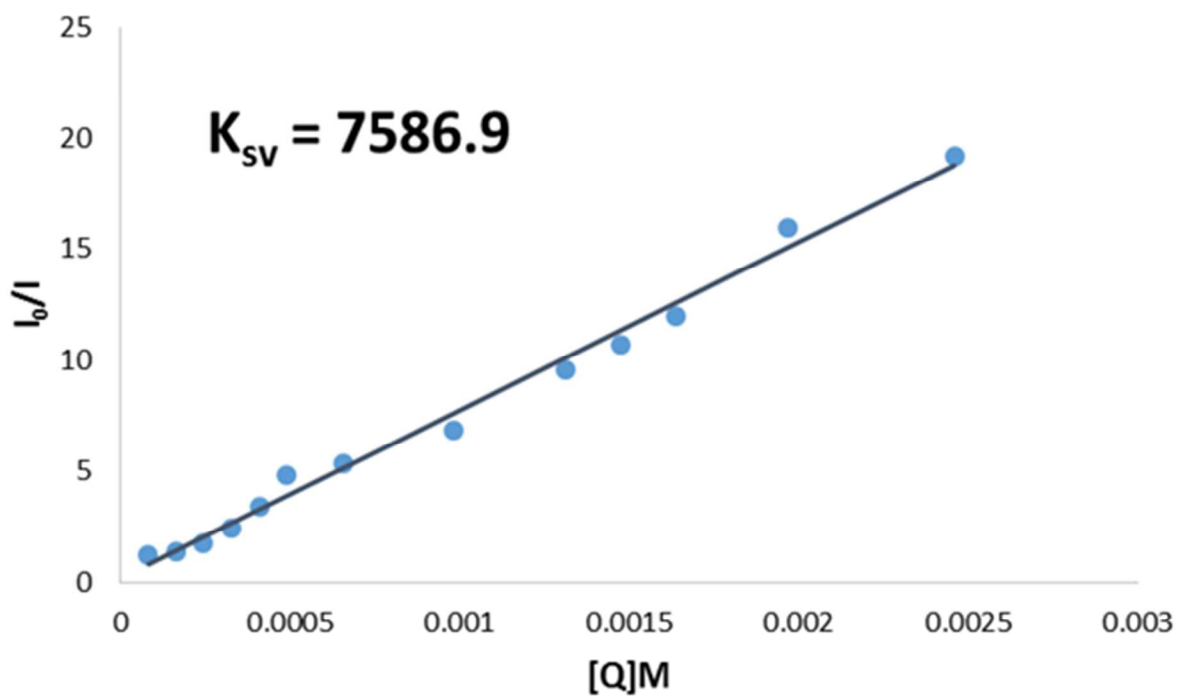
(b)



(c)



(d)



(e)

Figure S26. Stern–Volmer (SV) plots in the presence of 1 mg of **TMU-32** in different **NB** (a) **1,3-DNB** (b) **2,4-DNT** (c) **TNT** (d) **NM** (e) concentrations ($[Q]$) in toluene.

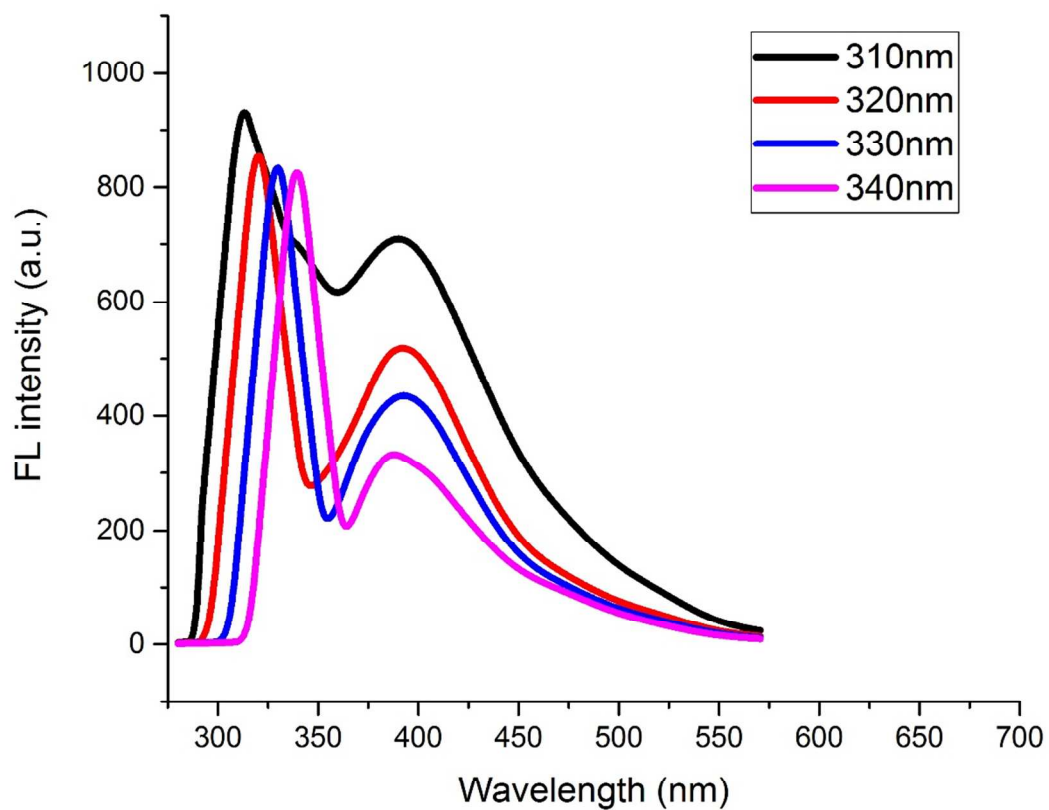


Figure S27. Fluorescence emission spectra of Dimethylformamide (DMF) upon excitation at 310, 320, 330 and 340 nm. The close matching of excitation and emission bands of DMF to that of TMU-31 and TMU-32 explains the intensification of emission in the presence of DMF.

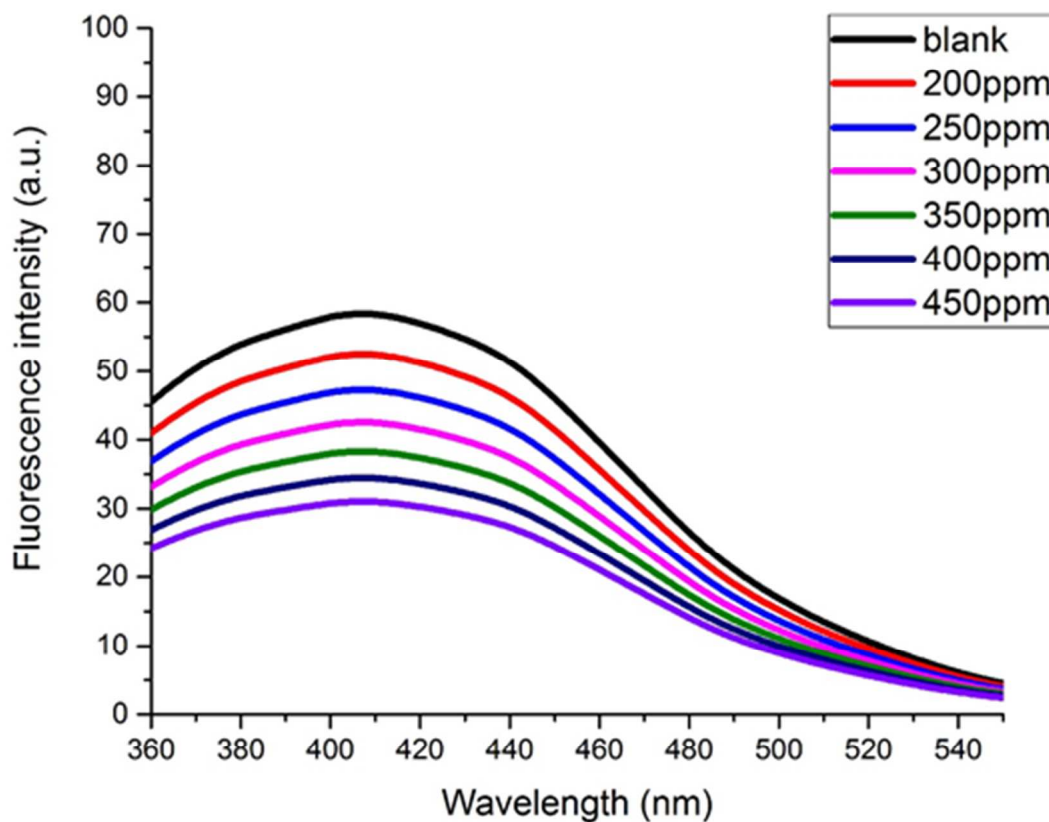


Figure S28. Fluorescence emission spectra of **TMU-31** dispersed in acetone solution at different concentrations of **NB**, excited at 320 nm.

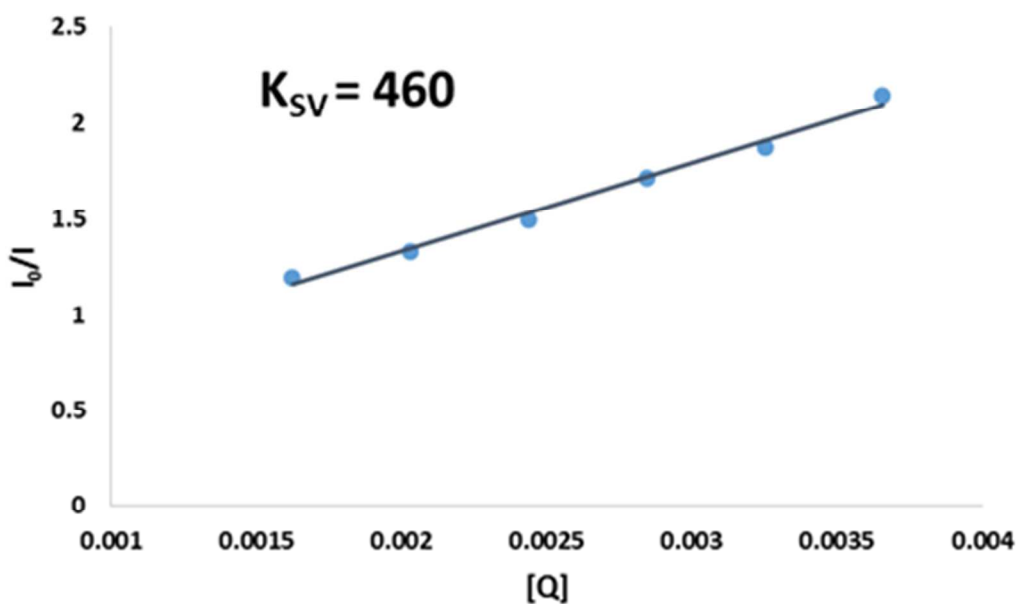


Figure S29. Stern-Volmer (SV) plots in the presence of 1 mg of **TMU-31** in different **NB** concentrations ($[Q]$) in acetone.

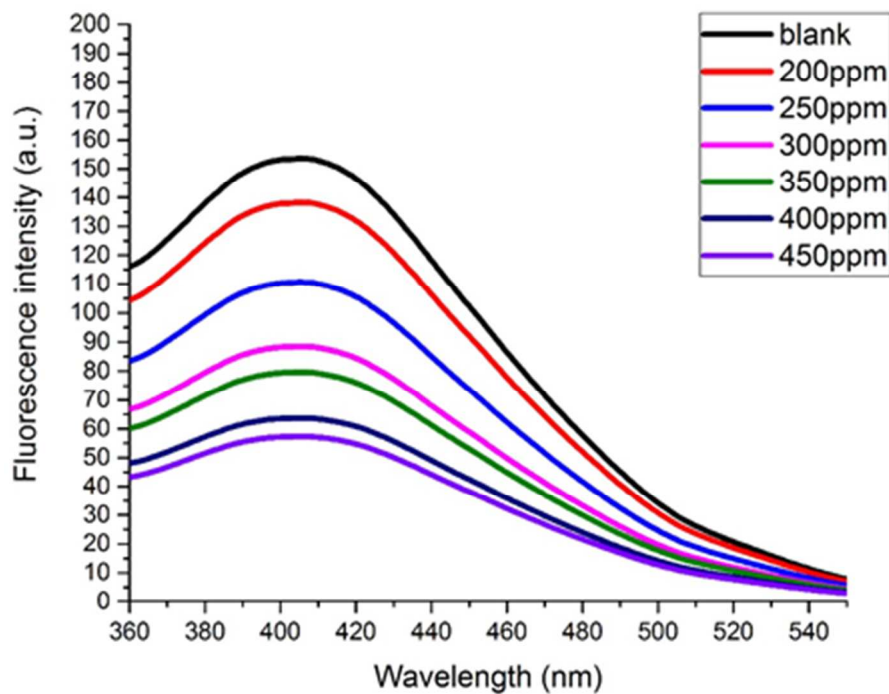


Figure S30. Fluorescence emission spectra of **TMU-32** dispersed in acetone solution at different concentrations of **NB**, excited at 320 nm.

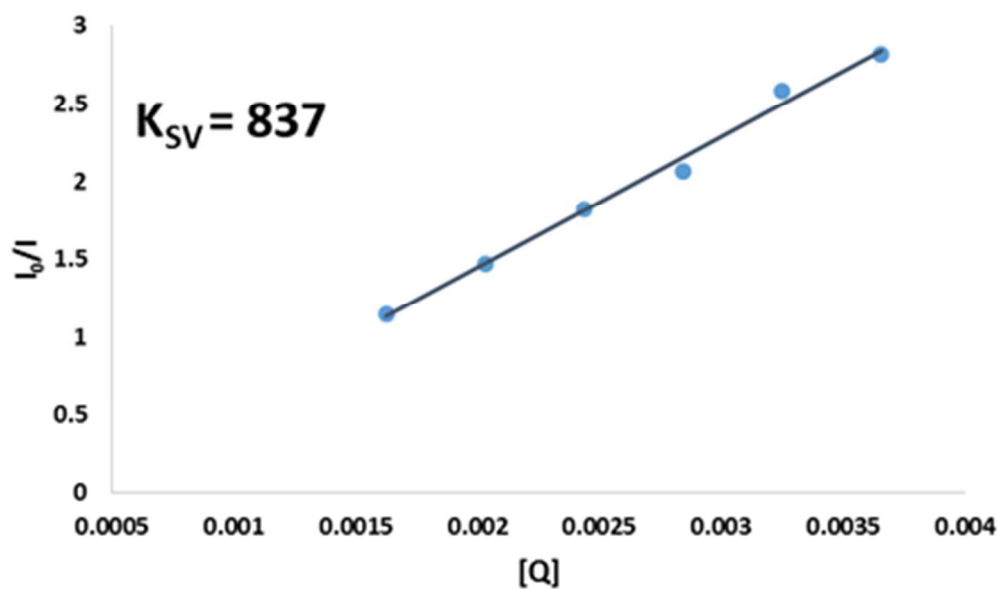


Figure S31. Stern-Volmer (SV) plots in the presence of 1 mg of **TMU-32** in different **NB** concentrations ($[Q]$) in acetone.

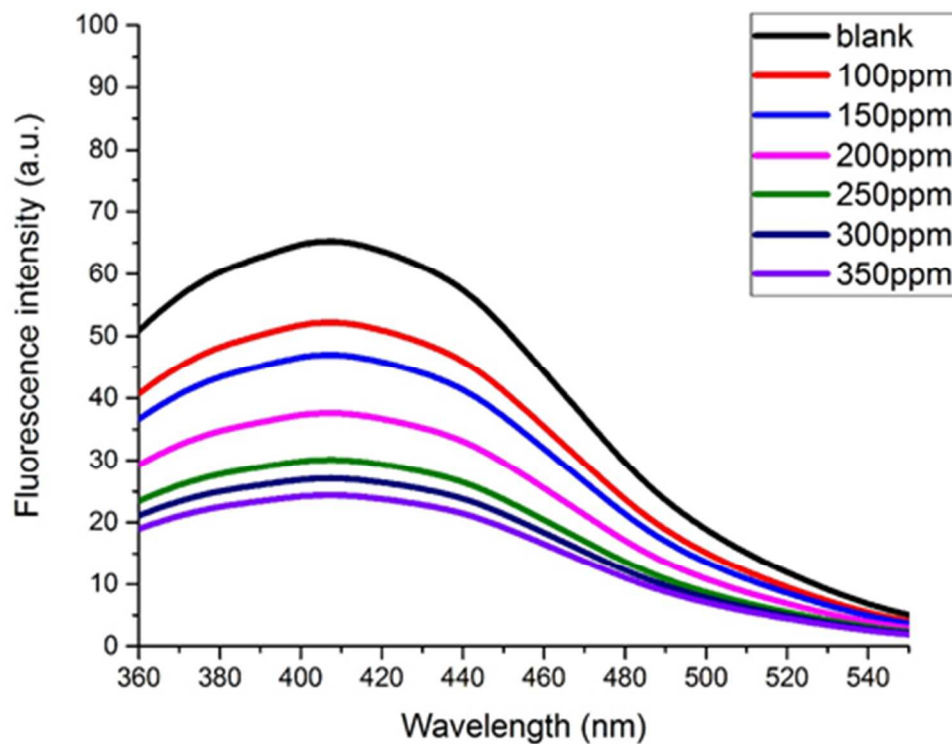


Figure S32. Fluorescence emission spectra of TMU-31 dispersed in acetone solution at different concentrations of DNB, excited at 320 nm.

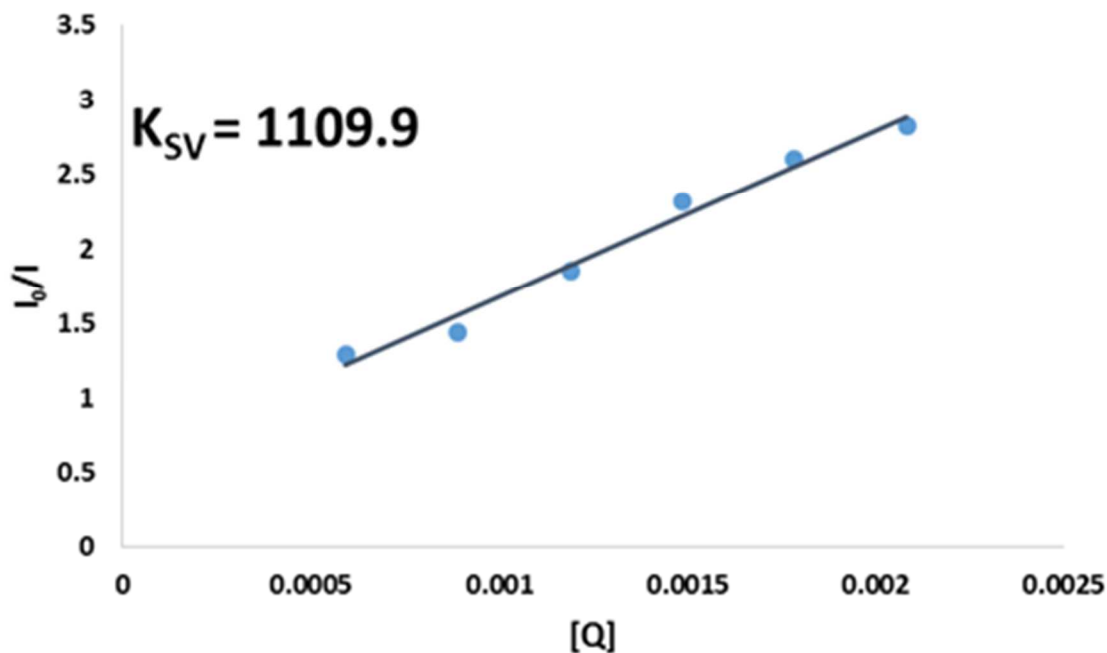


Figure S33. Stern–Volmer (SV) plots in the presence of 1 mg of TMU-31 in different DNB concentrations ($[Q]$) in acetone.

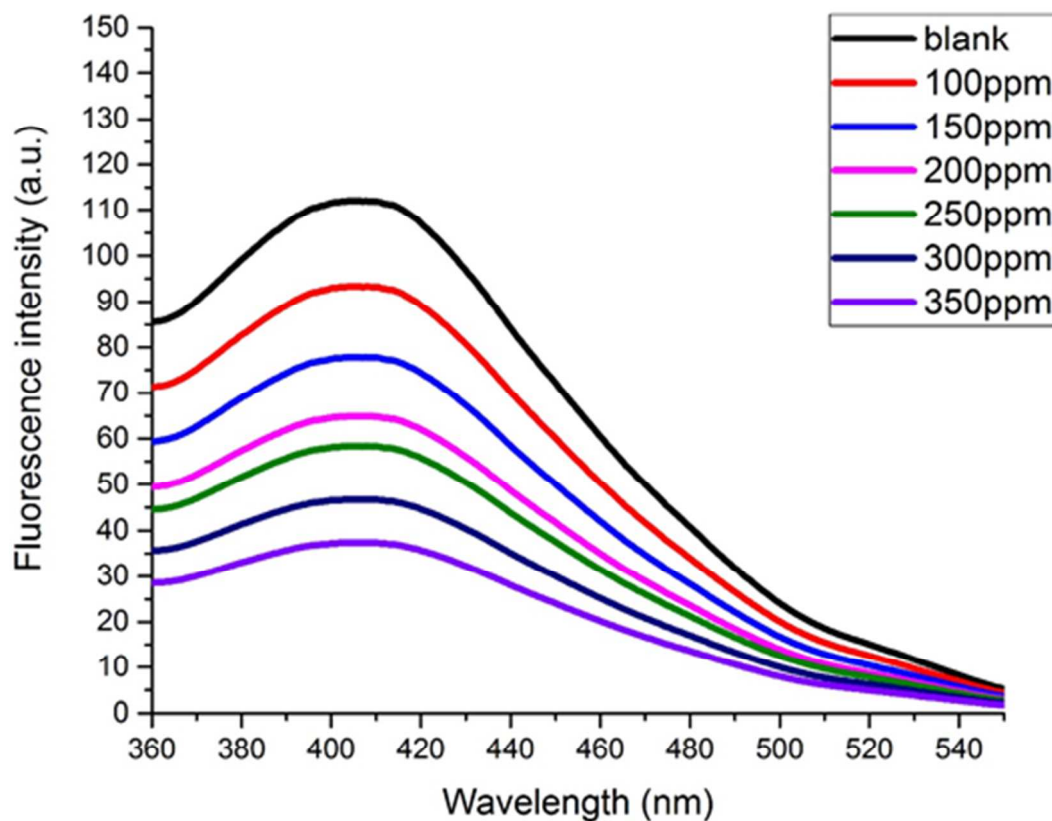


Figure S34. Fluorescence emission spectra of **TMU-32** dispersed in acetone solution at different concentrations of **DNB**, excited at 320 nm.

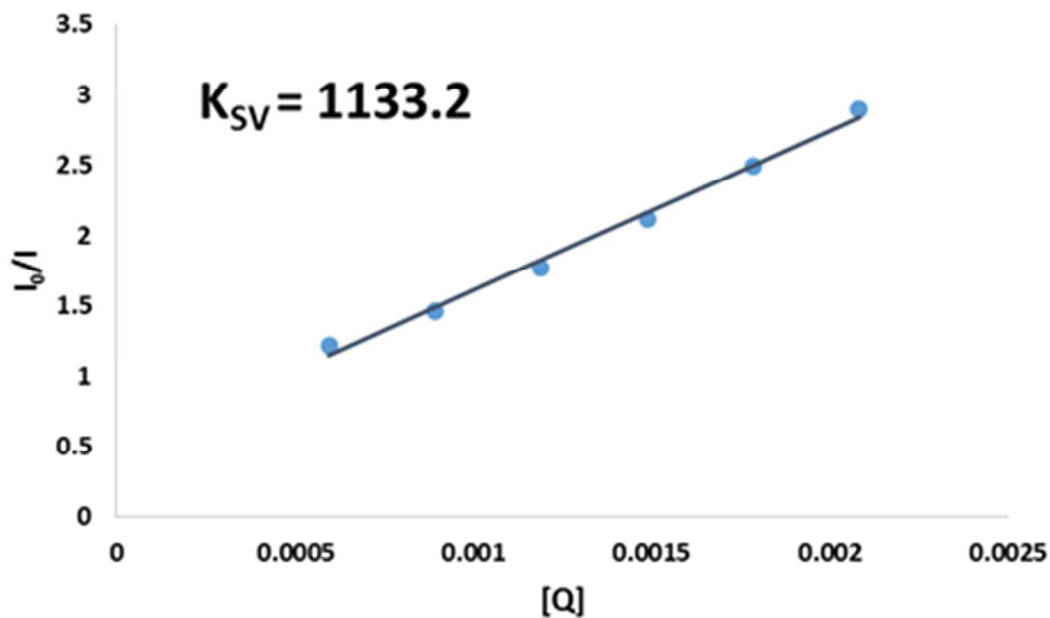


Figure S35. Stern–Volmer (SV) plots in the presence of 1 mg of **TMU-32** in different **DNB** concentrations ($[Q]$) in acetone.

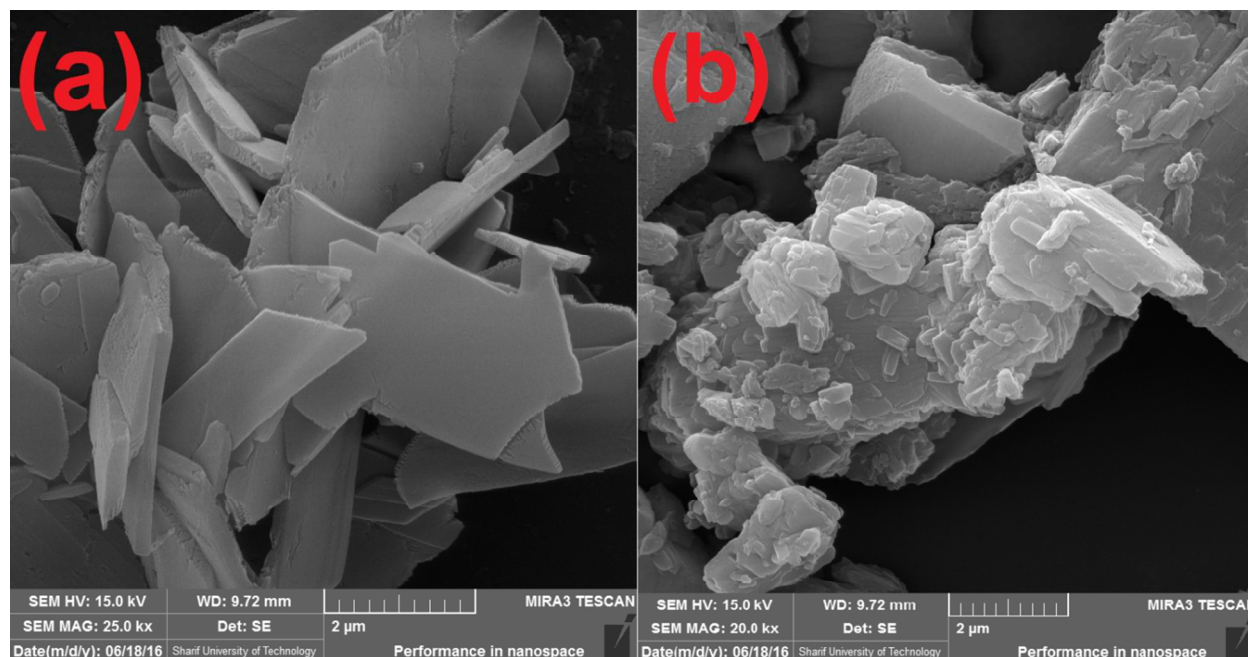


Figure S36. FE-SEM images of TMU-31 as-synthesized particles (a) after sensing (b)

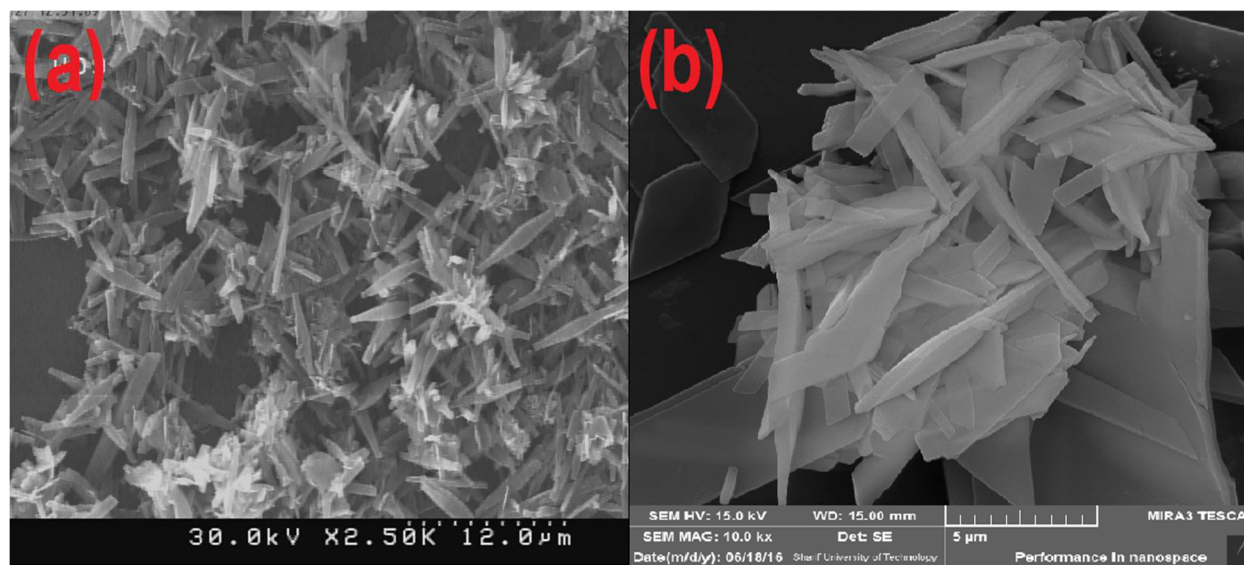


Figure S37. FE-SEM images of TMU-32 as-synthesized particles (a) after sensing (b)

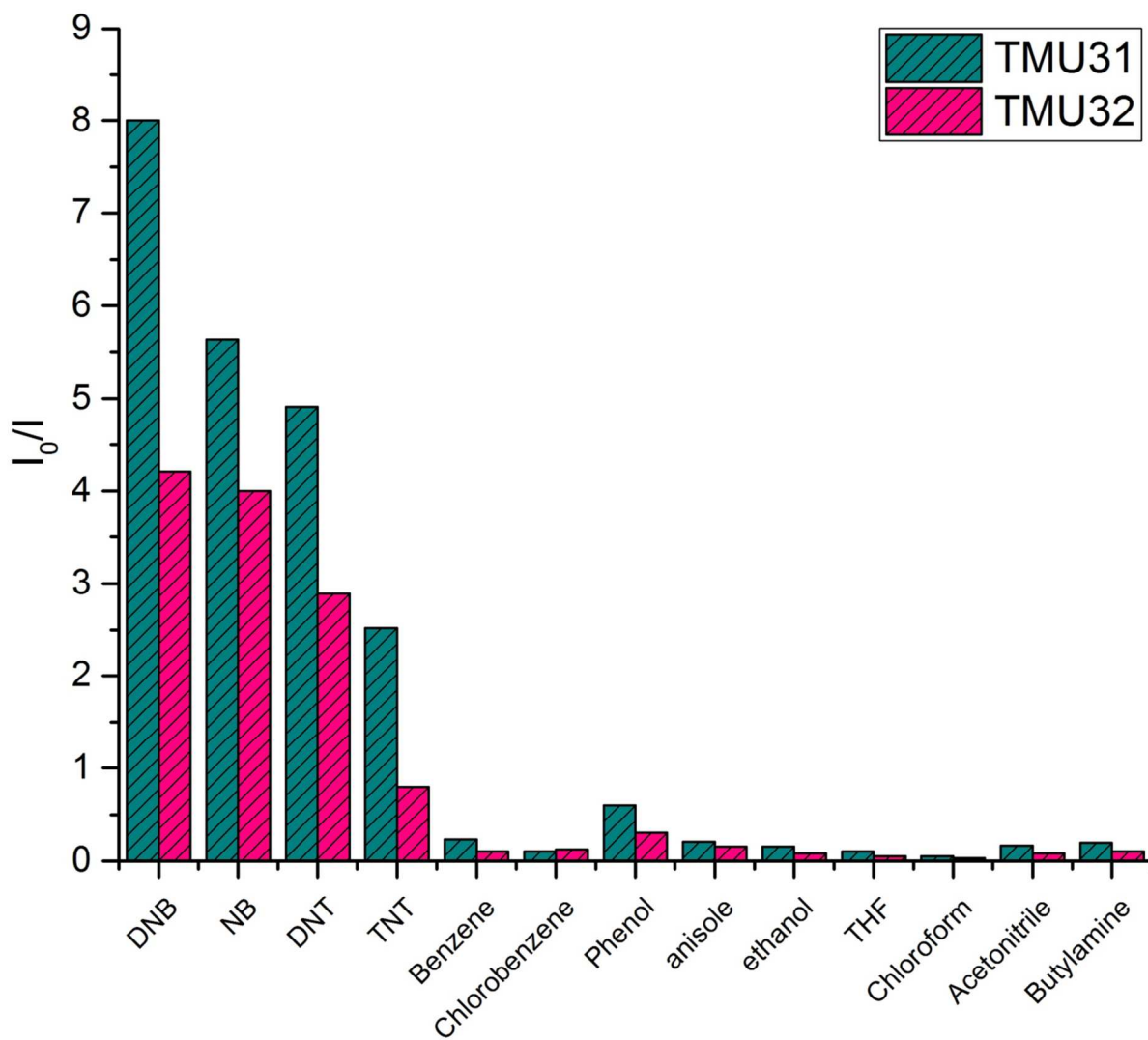


Figure S38. Relative fluorescence response of TMU-31 and TMU-32 to 60 ppm of different organics in toluene.

Extraction Procedure

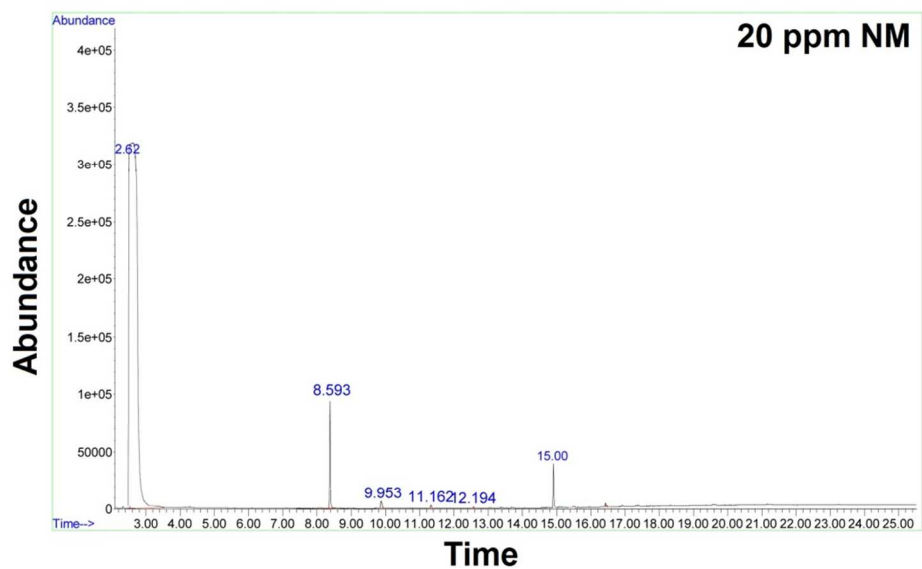
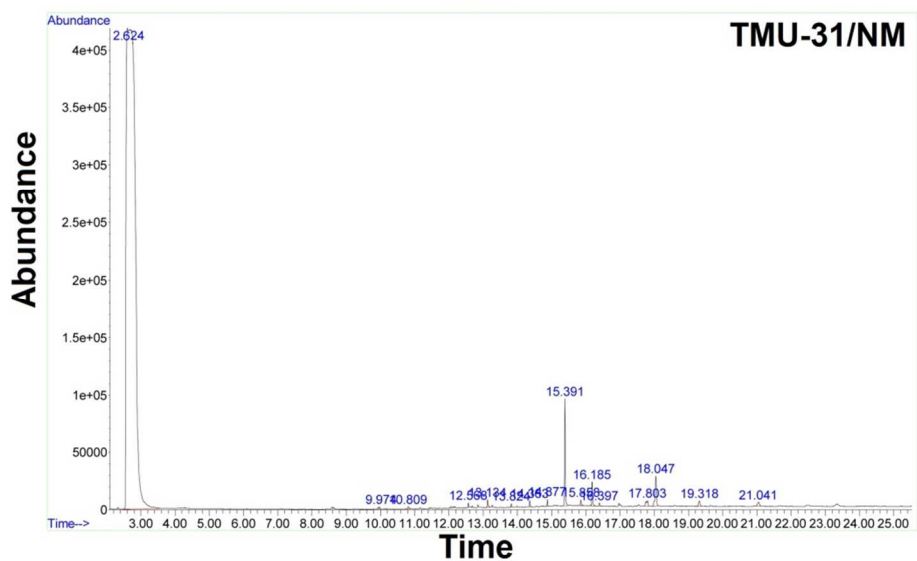
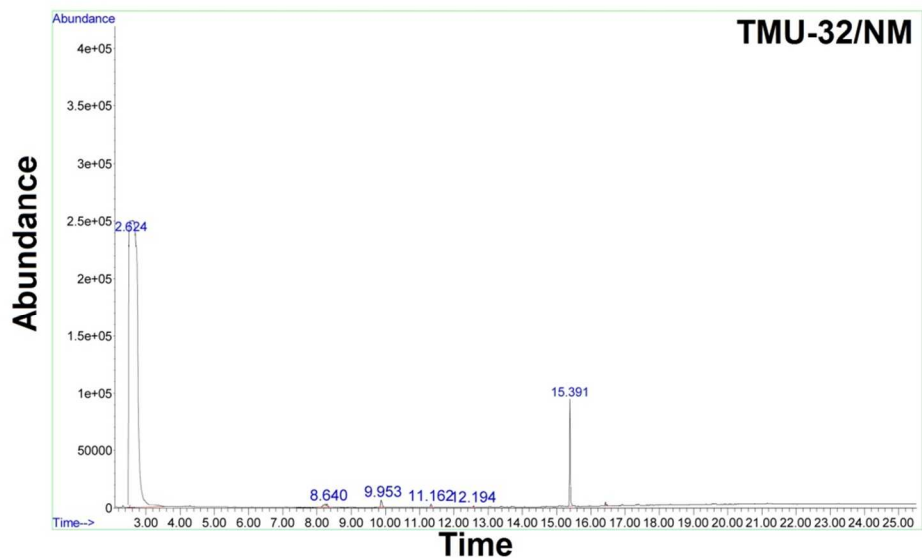
The procedure for the solid-phase extraction of nitrobenzene (NB) and nitromethane (NM) was according to the following steps: Initially a 10 mL toluene solution including 500 ppb of NB/NM, was added to a capped vial containing 3 mg of the MOFs as sorbent. After stirring for 15 min (in order to enhance the speed of adsorption), The sorbent was separated from the samples by centrifugation (6000 rpm for 2 min) and then washed with methanol to remove the physically adsorbed species on the sorbent surface. The analytes were desorbed from the sorbent with 1 mL of methanol by powerful vortex for 5 minutes. The extracts were further concentrated under a gentle stream of nitrogen gas to 100 μ L prior to GC-MS analysis, and 10 μ L of eluate was injected and analyzed by GC-MASS. The extraction efficiency was calculated according to the equation:

$$ER(\%) = \left(\frac{C_f V_f}{C_0 V_0} \right) \times 100$$

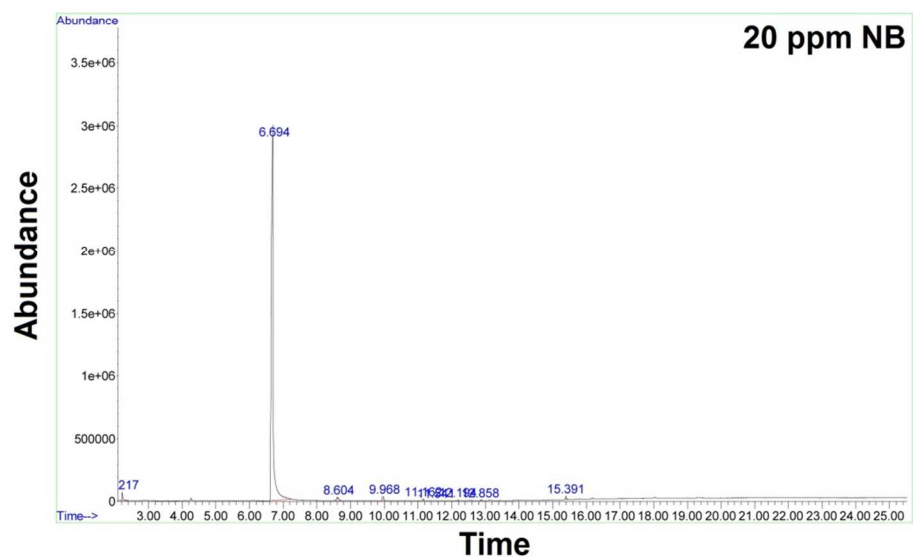
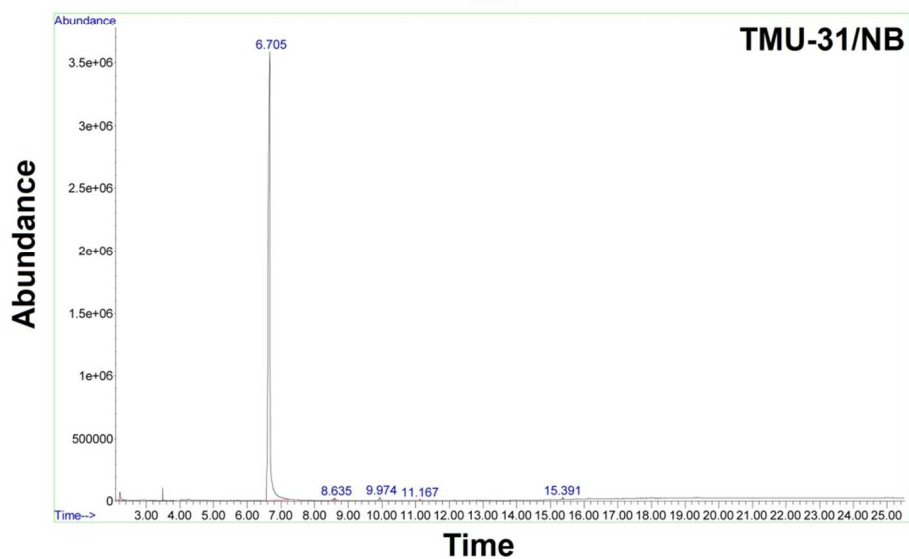
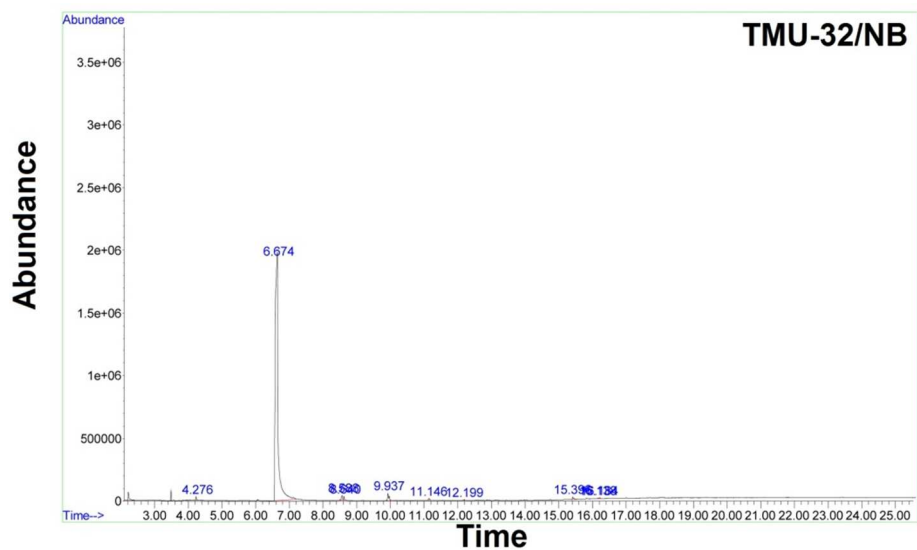
Where C_0 and C_f denote the initial concentration of the analyte in the sample solution and concentration of the analyte in the eluate after extraction with the proposed method, respectively, and V_0 and V_f are the volumes of the sample and the eluent, respectively.

Table S1. Comparison of Extraction Recoveries (ER) of **TMU-31** and **TMU-32**

Analytes	TMU-31	TMU-32
nitrobenzene	42.6	26.6
nitromethane	58.0	27.5



(a)



(b)

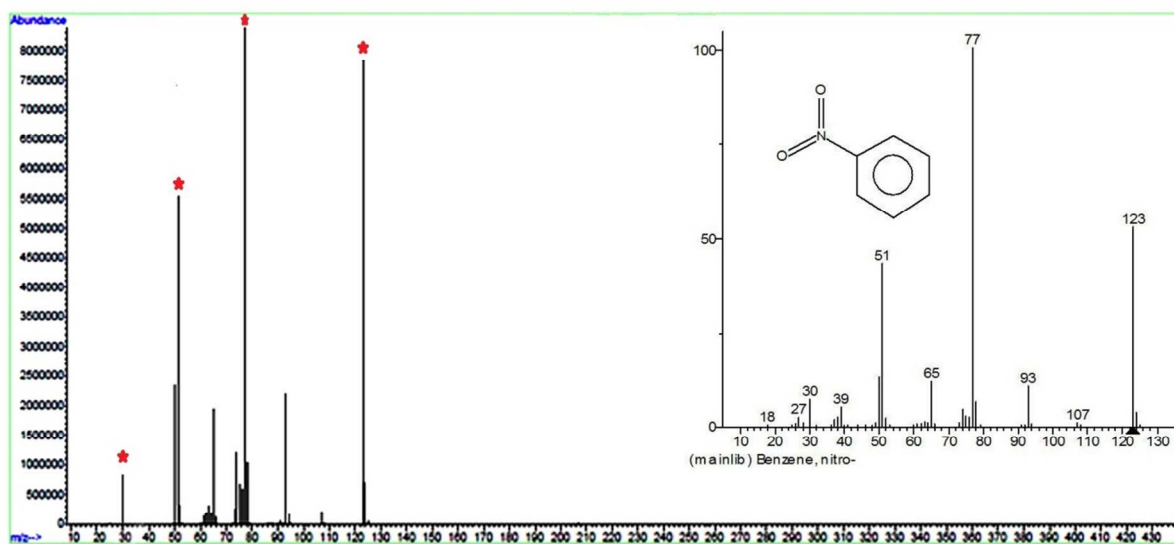
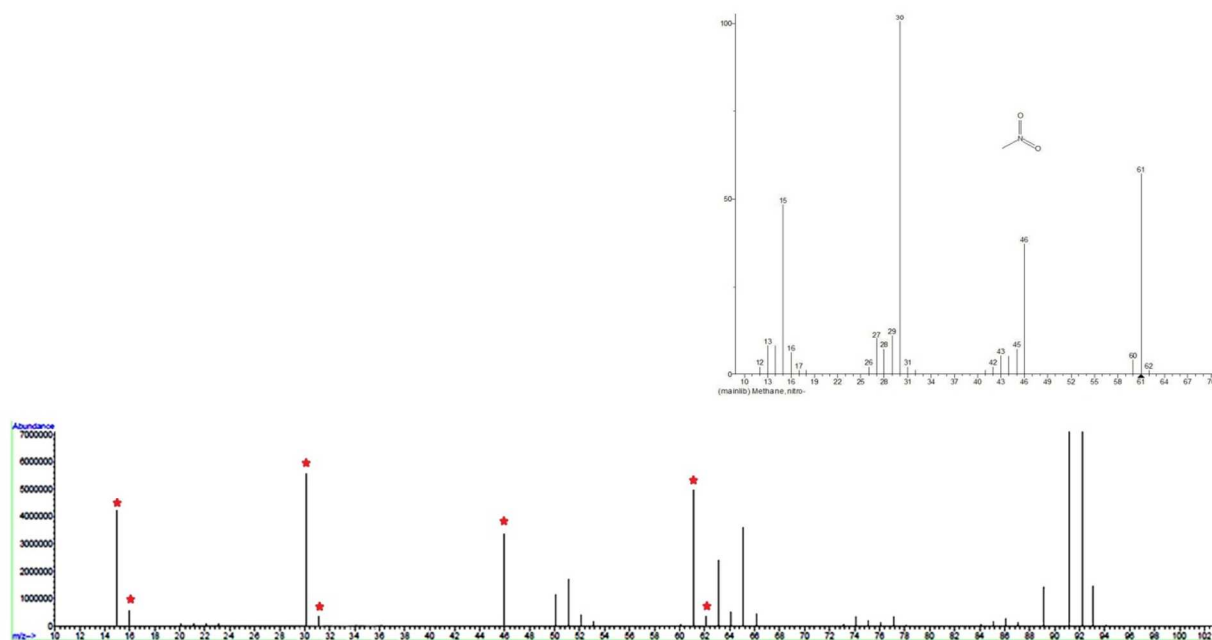


Figure S39. Extraction procedure. GC-Mass chromatograms (a for NM) and (b for NB) and mass analysis of extracts (c for NM) and (d for NB). In the case of nitromethane the signal at 92 is related to adsorbed toluene molecules.

Theoretical calculations

Since the urea group of L2 ligand in TMU-31 structure can be involved in nitroaromatics recognition, the ligand/NB, ligand/1,3-DNB, ligand/2,4-DNT and ligand/TNT were optimized using DFT method with B3LYP/6-31++G** with diffuse basis functions. The counterpoise corrected interaction energies (calculated at rb3lyp/6-31++g(d,p) level of theory) are shown in the following figures. The results show that urea group of L2 ligand and nitroaromatics interact mainly through N-H...O hydrogen bond to form a $R_2^2(8)$ hydrogen bonding synthon.

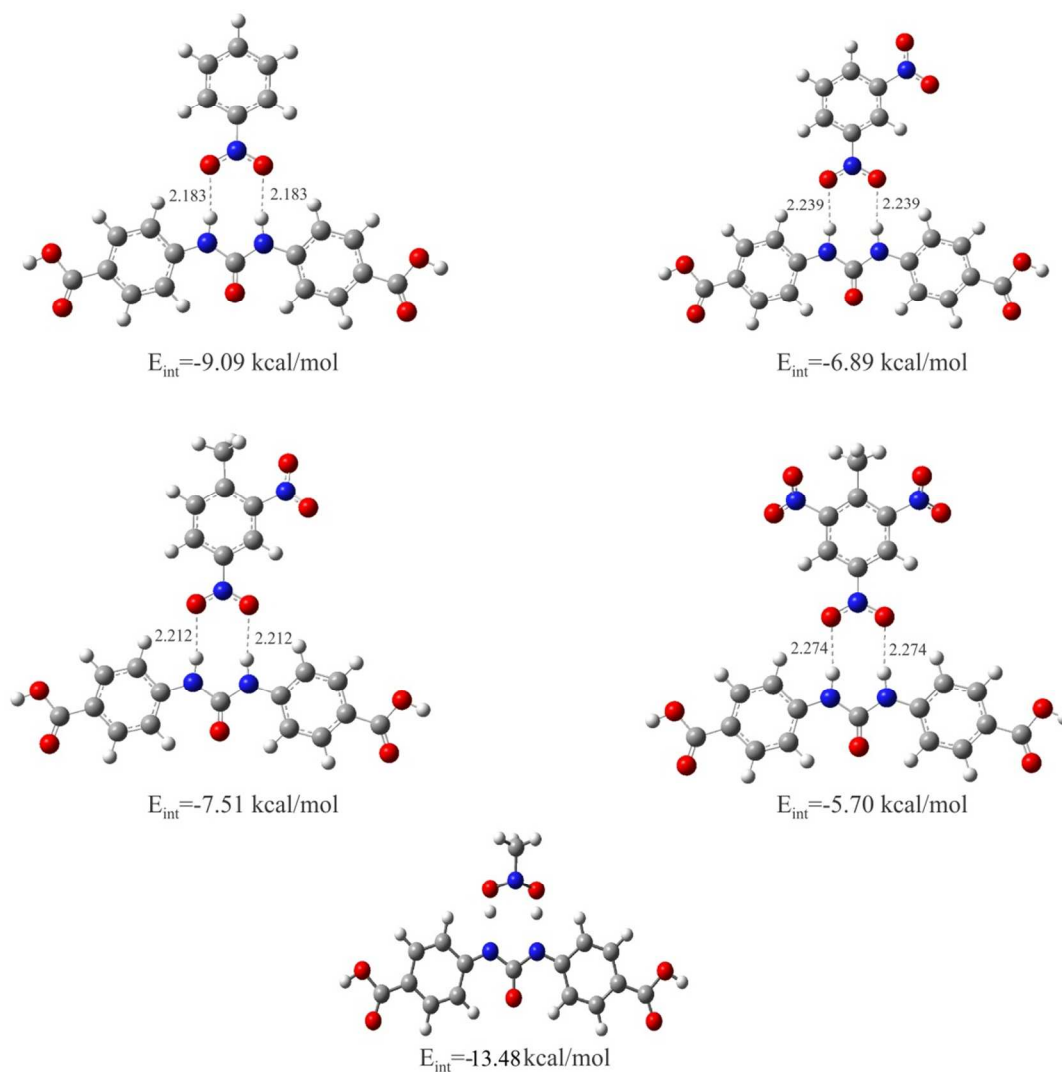


Figure S40. Interaction energies for urea-containing ligand L1 in the presence of nitroaromatics. It is to be noted that in the case of urea/nitromethane the binding energy is greater than other nitro-analytes and the urea hydrogen atoms are partially transferred to the oxygen atoms of nitromethane.

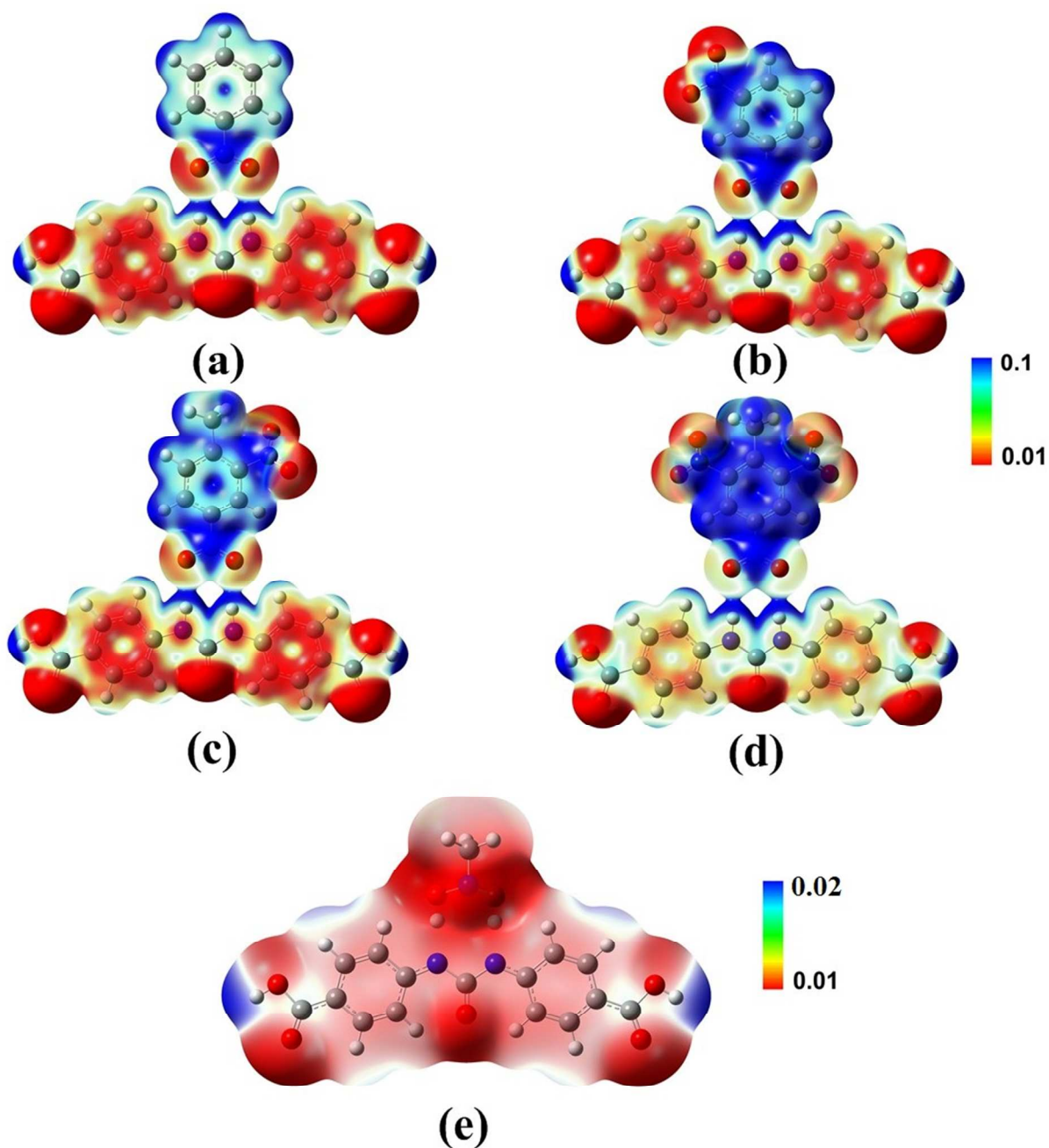


Figure S41. Electrostatic potentials mapped on the electron isodensity surface of ligand L1/NB (a) ligand L1/1,3-DNB (b), ligand L1/2,4-DNT (c) ligand L1/TNT (d) and L1/NM at the same contour value of 0.01 electron per Bohr³. The red color shows the most negative potential, while the blue color represents the most positive one (e).

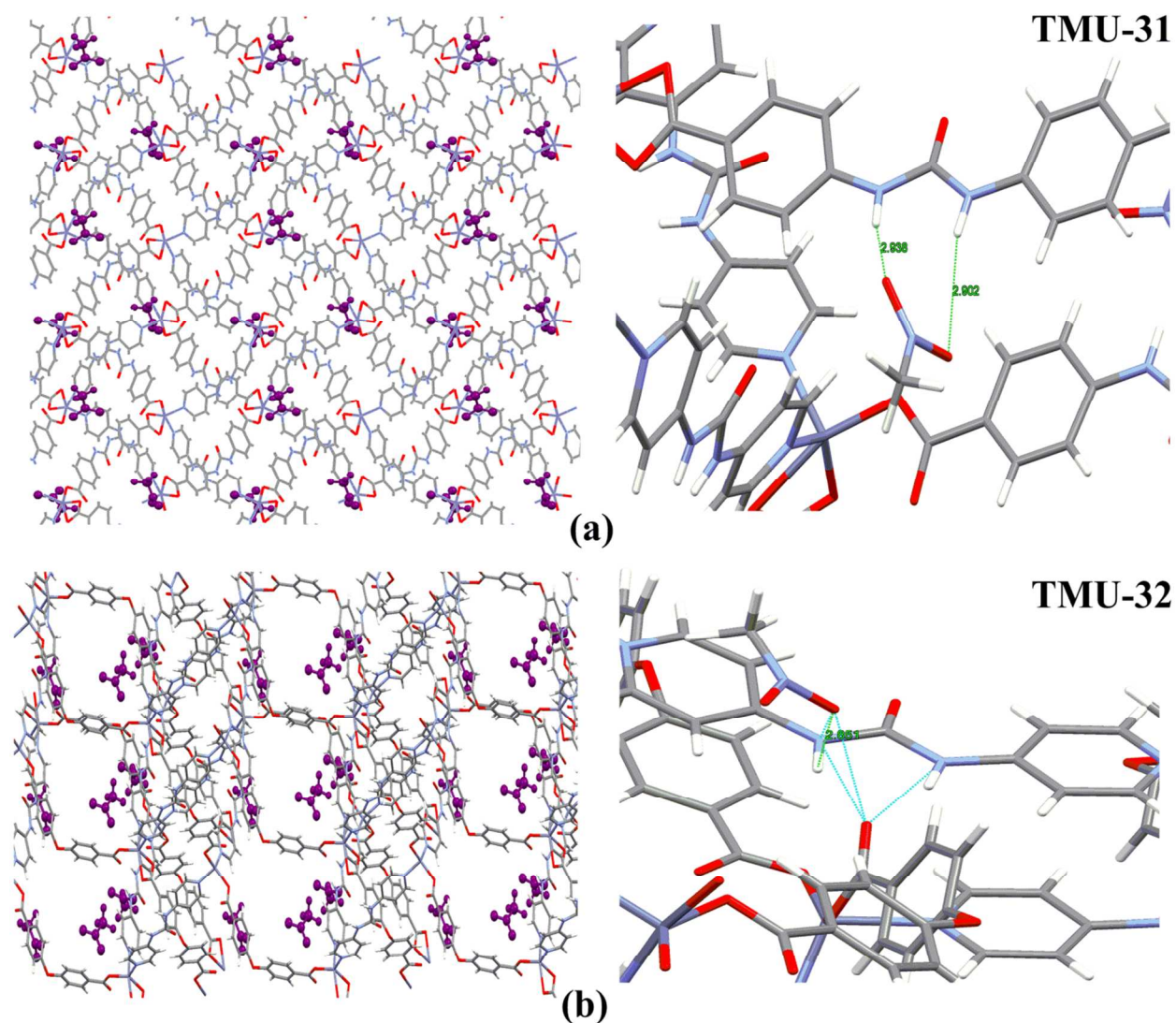
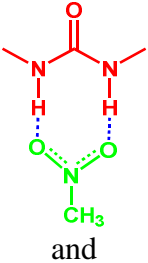
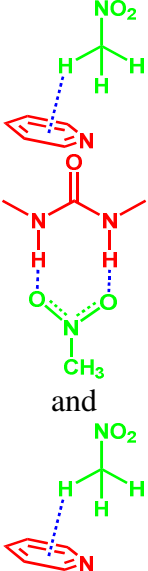


Figure S42. Orientation of nitromethane analytes in the pores of TMU-31 (a) and TMU-32 (b) and representation of urea-nitromethane interaction. The interaction between the host (MOFs) and the nitromethane guests was investigated by performing Monte Carlo simulations using the adsorption locator module in Accelrys Materials Studio. The simulation reveals that the probable adsorption site for nitromethane guests in these frameworks is near the urea functional group of L1 in TMU-31 and L2 in TMU-32.

Table S2. Details of adsorption analysis using adsorption locator module of Material studio.

MOF	Analyte	MOF-analyte Binding synthon	MOF-analyte interaction	Loading per unit cell	Total binding energy
TMU-31	Nitromethane		N-H...O Hydrogen bond and CH- π interactions	1	-13.95
				2	-27.60
				3	-41.62
TMU-32	Nitromethane		N-H...O Hydrogen bond and CH- π interactions	1	-10.44
				2	-21.79
				3	-28.01

References

- [1] McPhillips, T. M.; McPhillips, S. E.; Chiu, H. J.; Cohen, A. E.; Deacon, A. M.; Ellis, P. J.; Garman, E.; Gonzalez, A.; Sauter, N. K.; Phizackerley, R. P.; Soltis, S. M.; Kuhn, P., Blu-Ice and the Distributed Control System: software for data acquisition and instrument control at macromolecular crystallography beamlines. *J. Synchrotron Rad.* **2002**, *9*, 401-406.
- [2] Kabsch, W. *J. Appl. Cryst.*, Automatic processing of rotation diffraction data from crystals of initially unknown symmetry and cell constants. **1993**, *26*, 795-800.
- [3] Sheldrick, G. M. *SHELXL-97* Program for crystal structure refinement, University of Gottingen, Germany, **1997**.
- [4] Barbour, L. J. *J. Supramol. Chem.*, X-Seed—A software tool for supramolecular crystallography. **2001**, *1*, 189-191.
- [5] Dolomanov, O. V.; Bourhis, L. J.; Gildea, R. J.; Howard, J. A. K.; Puschmann, H., OLEX2: a complete structure solution, refinement and analysis program. *J. Appl. Cryst.* **2009**, *42*, 339-341.